A Delta-V Map of the Known Main Belt Asteroids

Anthony Taylor
Harvard University

Abstract

With the lowered costs of rocket technology and the commercialization of the space industry, asteroid mining is becoming both feasible and profitable. Although the first targets fore mining will be Near Earth Asteroids (NEAs), the Main Belt contains 10^6 times more material by mass.. The creation and expansion of this new asteroid mining industry is contingent on minimizing the cost to match orbits and rendezvous with Main Belt asteroids, dictated by the necessary velocity change in a mining spacecraft (Delta-V). This paper develops two different flight burn paths, both starting from Low Earth Orbit (LEO) and ending with successful rendezvous. These methods are then applied to the 700,000 asteroids in the Minor Planet Center database to analyze the Main Belt asteroids to find low Delta-V mining targets. We find that there are 5,211 potential targets with a Delta-V < 8 km s^{-1}, but the distribution is steep and reduces to 7 with Delta-V < 7 km s^{-1}. We then compare the strengths of the two burn methods.

1. Introduction

For decades, asteroid mining has been largely dismissed as infeasible and unprofitable. However in recent years, a combination of technological and economic factors have injected new realism into the field, and for the first time, these hint at a distinct possibility of reliable, profitable, and large scale asteroid mining, as well as human exploration and science initiatives.

Technologically, the next generation of rockets is in development. Projects such as SpaceX's Falcon Heavy and Blue Origin's New Glenn should serve to

greatly decrease mission costs. Mission cost is vital to the success of asteroid mining, as cost clearly affects the profitability of commercial missions.

Economically, the space industry has undergone a great change in recent years. With the privatization of the industry, commercial organizations no longer need to rely solely on government programs such as NASA to reach Earth orbit and beyond. The introduction of Elon Musk's SpaceX, Jeff Bezos' Blue Origin, and other private space firms has turned the space market into a competitive sphere. Such an environment is a prime catalyst in reducing the cost of space missions including asteroid mining. Mining could be a major market for space firms, potentially providing a wide customer base to drive and sustain the industry.

The base principle of asteroid mining is to launch a vehicle from Earth that rendezvouses with a target asteroid. After rendezvous, the vehicle extracts economically valuable material from the asteroid such as precious metals (gold, platinum, etc), construction materials (iron, aluminum, copper), and/or water for use in space [4]. After mining, the spacecraft delivers its cargo either back to Earth, or to a more exotic location such as a high Earth Orbit, the Moon, Mars, or a crewed spacecraft.

The critical factor in the asteroid mining market is that the cost per kilogram of mined material must be significantly higher than the transport costs. While the demand for precious metals on Earth is clear (especially for industrial applications for platinum and gold), they are hard to extract. Construction materials and especially water are much easier to extract, but their value depends on future off-planet projects, where the cost of shipping such materials from Earth could be much higher than importing them from asteroids.

The first step in the creation of this new industry is an examination of known asteroids to find profitable, easy to reach targets. While the $\sim$15,000 known Near-Earth Objects (NEOs) have already been analyzed [5], the asteroid Main Belt between Mars and Jupiter has not received major attention. While the Main Belt asteroids are certainly further away and mostly more costly to access in propellant, the sheer number of known objects (over 700,000 compared

to around 15,000 NEOs[1], with over 10^6 times as much mass [4]) offers great possibilities for the developing industry. Here we seek to identify within this plethora of objects, those asteroids that are most accessible, resulting in new targets for this nascent industry.

The energy costs of reaching an asteroid are crucial. The rocket equation [5] imposes an exponential penalty in mass for a linear change in energy cost. The energy cost is measured in Delta-V, the total velocity change that a spacecraft must undergo to match orbits and rendezvous with another body, in this case, an asteroid. The rocket equation is given by:

$$\Delta V = v_e \ln\left(\frac{m_i}{m_f}\right) \tag{1}$$

Where ΔV is Delta-V, v_e is the velocity of the rocket's exhaust, m_i is the rocket's initial mass, and m_f is the rocket's final mass [6]. This equation governs the ratio of wet (with propellant) to dry (propellant excluded) mass of a spacecraft with a given Delta-V rating, limiting the mass of equipment that a spacecraft can carry on a mission. Solving for this ratio gives:

$$\frac{m_i}{m_f} = \exp\left(\frac{\Delta V}{v_e}\right) \tag{2}$$

This demonstrates that a linear change in Delta-V causes an exponential change in the necessary propellant for a mission. Or, for a fixed capability rocket, the delivered payload in reduced comparably. Thus, we seek to minimize the Delta-V for a mission so as to reserve more mass for equipment and flight systems.

This paper is organized as follows:

- Section 2: Orbital Mechanics - Overview of the mechanics used in deriving the orbital burns
- Section 3: Multiple Burn Approaches - Discussion of different sets of orbital burns
- Section 4: The 3 Burn Method - Derivation of the first orbital burn method

[1] http://www.minorplanetcenter.net/iau/MPCORB/NEA.txt

- Section 5: The 2 Burn Method - Derivation of the second orbital burn method
- Section 6: Data Analysis - Application of the orbital burn methods to the Main Belt dataset
- Section 7: Results and Analysis - Discussion of the Delta-V results, and a comparison of the two methods
- Section 8: Conclusions and Future Directions - Summary of the investigation results and relevant future projects

2. Orbital Mechanics

In this analysis, we use the Patched Conics approximation of orbital mechanics, in which the orbiting object is gravitationally affected by only one gravity well at a time[2] [8]. Such an orbit, known as an Osculating Orbit, is characterized by a series of parameters or "orbital elements" [3]. These are derived from Kepler's Laws of Planetary Motion, and when all are known, an objects's orbit and position on its orbit is completely determined. The six elements are the semimajor axis a, eccentricity e, argument of the periapsis ω, inclination i, longitude of the ascending node Ω, and true anomaly ν at epoch ν_0. Figure 1 shows these parameters graphically. There are defined as follows:

- Semimajor axis (a): Half of the distance between the highest and lowest points above the center of mass of the central object.
- Eccentricity (e): Kepler's first law defines planetary orbits as conic sections [10]. The eccentricity of an orbit corresponds to the eccentricity of the orbital conic section.

[2]For example, in patched conics, an object orbiting Earth will only be subject to Earth's gravity, with no interference from the Sun or Moon. Similarly, an object in a solar orbit will be affected only by the Sun, ignoring the gravitational effects of the Planets and all other objects.

- Inclination (i): The angle between the orbital plane and a reference plane (usually, and here, defined as Earth's orbital plane around the Sun, the ecliptic).

- Longitude of the Ascending Node (Ω): The Ascending Node is one of two (with the Descending Node) intersection points of the orbital plane and the reference plane. The Longitude of the Ascending Node is the angle measured in the reference plane between an arbitrary reference direction and the Ascending Node.

- Argument of the Periapsis (ω): The angle measured in the orbital plane from the Ascending node to the periapsis (defined below) of the orbit.

- True Anomaly (ν) at Epoch (ν_0): The angle in the orbital plane between the periapsis and the position of the orbiting object at the given time known as the epoch (J2000, B1950, etc). The True Anomaly while not at epoch is given by ν.

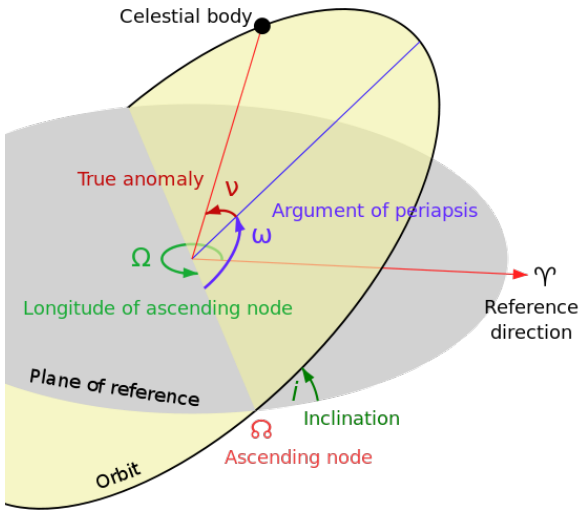

Figure 1: Illustration of the angular orbital elements.
(By Lasunncty (Wikipedia Contributer), CC BY-SA 3.0.
https://commons.wikimedia.org/w/index.php?curid=8971052)

In addition to the six traditional orbital elements and the epoch, other derived elements are useful in calculations.

- Apoapsis: The point on an orbit that is furthest from the central object.
- Periapsis: The point on an orbit that is nearest to the central object.
- Ecliptic Latitude: The angle between a point on the orbit and the ecliptic plane

The Keplerian equations for orbital motion are given as follows [10]:

$$r(\nu) = \frac{a(1-e^2)}{1+e\cos(\nu)} \tag{3}$$

Eq. (3) gives the radius r, or distance between the central object and the orbiting object as a function of true anomaly ν.

$$v(r) = \sqrt{\mu\left(\frac{2}{r} - \frac{1}{a}\right)} \tag{4}$$

Eq. (4) gives the orbital velocity of an object as a function of the object's current orbital radius. Here, μ is the standard gravitational parameter and is defined as Newton's gravitational constant G multiplied by the mass of the central object M.

$$\mu = GM \tag{5}$$

These equations and elements, along with vector algebra serve as the basis of our calculations. This Keplerian approach uses purely classical mechanics and does not take into account the effects of special or general relativity. Fortunately, for at reasonable distances from the Sun (at the Earth's orbit or beyond) the effects of general relativity on solar orbits are entirely negligible.

Orbital changes are achieved through the operation of reaction engines in a series of burns. We do not consider continuous low-thrust regimes, such as ion engines [2] in this work. Instead we assume that all burns are performed with a high thrust engine, approximating that all changes in velocity due to burns are instantaneous. Each burn will change the orbital velocity vector of

the spacecraft, thereby changing its orbit. The six orbital elements provide six degrees of freedom in an orbit. In this six parameter space an alternate set of parameters to use could be an (x, y, z) position vector and a (v_x, v_y, v_z) velocity vector. These six elements can also completely characterize an orbit and an object's position on the orbit. Thus, when a spacecraft executes a burn, it changes its velocity vector and modifies its orbit.

2.1. Delta-V

This manipulation of the velocity vector gives rise to the concept of Delta-V (ΔV). As previously stated, Delta-V is defined as the change in velocity that a spacecraft undergoes during a burn or a mission. The Delta-V of a rocket plus spacecraft determines the total potential velocity change of the spacecraft that is achievable during burns over the course of a mission. Hence higher Delta-V implies that a spacecraft can travel to more difficult to reach targets.

In this paper, Delta-V to a celestial object is defined as the total amount of velocity change necessary for a spacecraft to rendezvous with this object. In this examination of the Main Belt asteroids, we are searching for the asteroids with the lowest Delta-V, as they can be reached more easily with current and future spacecraft.

The Delta-V required to reach a target is highly dependent upon the target's orbit. There is no unique set of burns necessary to reach a target, rather, any number of different burns can be used for a successful rendezvous. To rendezvous with an asteroid, the spacecraft must match both its velocity and position (and therefore its orbit) vectorially. This differs from a rendezvous with a planet or other large body, as the gravity of the target object is then much larger than that of an asteroid, requiring at least entry into a capture orbit, and a controlled descent, if desired. For a Main Belt asteroid, even the most massive Ceres ($g_{Ceres} = 0.03$ g) [9], the effects of the asteroid's gravity are negligible for Delta-V calculations.

3. Multiple Burn Approaches

The restrictions on spacecraft design imposed by the rocket equation motivate the search for the set of burns requiring the least amount of Delta-V to reach a given target. Achieving the optimal Delta-V to a specific target is dependent on that target's specific orbit. Thus for a large dataset of objects with diverse orbital characteristics, a single chosen set of orbital burns will not have the absolute lowest Delta-V to the object, at the same burns must be easily adapted and applied to the entire dataset.

For a successful rendezvous starting from the Earth, a space craft must execute a minimum of two burns to reach a Main Belt Asteroid, one to escape the Earth, and one match orbits with the target asteroid. The spacecraft may perform additional burns additional burns depending on the flight plan, but two is the absolute minimum for an asteroid that does not cross the Earth's orbit.

While early studies of NEOs [5] use the Shoemaker-Helin Equations [11], these equations were developed for use with NEOs and Earth Crossing Asteroids and as a result make approximations that may not hold to sufficient precision and efficiency for Main Belt targets. For example, the Shoemaker-Helin equations disregard the target asteroid's argument of periapsis ω, which is important for a precise rendezvous.

In response to this, we have developed two different series of burns capable of achieving rendezvous with Main Belt asteroids, each with its own strengths and efficiencies. The first uses 3 burns, the second uses 2 burns. Both methods assume that the spacecraft starts in a circular equatorial parking orbit around the Earth, and are designed to end with a successful asteroid rendezvous. The principles of each are described below.

3 Burn Method

1. *Burn 1* is performed when the ecliptic longitude of the Earth is 180 degrees from the ecliptic longitude of the asteroid at apoapsis. Burn 1 must also be performed at a time such that both the spacecraft and the asteroid

will reach the asteroid's apoapsis at the same time (this will decrease the Delta-V necessary for Burn 3, as explained later). Burn 1 will cause the spacecraft to escape Earth with a velocity in excess of the required escape velocity, such that the apoapsis of the spacecraft above the Sun is the same distance and ecliptic longitude as the apoapsis of the asteroid. The orbit of the spacecraft after Burn 1 is in the ecliptic, but it is now much more eccentric.

2. *Burn 2* is performed at true anomoly $\nu = 90°$ relative to the argument of the periapsis of the asteroid ω. Burn 2 changes the direction but not the magnitude of the spacecraft's velocity, rotating the velocity vector and orbital trajectory out of the ecliptic plane. This rotation is performed such that the apoapsides of the spacecraft and asteroid coincide in 3D space. The location of the spacecraft at the time of Burn 2 then defines the ascending or descending node of the spacecraft transfer orbit, depending upon whether the burn causes the spacecraft to move toward positive or negative ecliptic latitudes. Through the proper planet/asteroid alignment in Burn 1, after Burn 2 the spacecraft and the asteroid will arrive at the same place at the same time.
3. *Burn 3* is executed near the time when the spacecraft encounters the asteroid at apoapsis. At initial approach the spacecraft and the asteroid will have different velocity vectors. Burn 3, by design, is the vector velocity (magnitude and direction) that must be added to the spacecraft velocity so that it matches that of the asteroid, thereby matching their orbits and achieving rendezvous.

2 Burn Method

1. *Burn 1* is identical in function to Burn 1 in the 3 Burn Method, except that the alignment is different. In the 2 Burn Method, Burn 1 is chosen to place the spacecraft's apoapsis at the ascending or descending node of the asteroid. The timing of the launch is chosen such that the spacecraft and asteroid reach that intersection point at the same time. As the ascending

and descending nodes are the only points of the asteroid's orbit that lie in the ecliptic (assuming non-zero inclination), this combines Burns 1 and 2 of the 3 Burn Method, causing the spacecraft and asteroid to be at the same position in space for the final burn.

2. *Burn 2* is performed at the apoapsis of the spacecraft transfer orbit established by Burn 1. By Burn 1's design and timing, this will also be the ascending or descending node of the asteroid's orbit, and the asteroid will also be at this position when Burn 2 is performed. Burn 2, like Burn 3 above, chooses the burn magnitude and direction to match the spacecraft and asteroid velocities, thereby achieving rendezvous.

Both methods achieve the same goal, but do so with different flight paths. The only time these flights paths would be that same is with an orbit with the argument of the periapsis ω of exactly $0°$ or $180°$. Such an orbit would cause the two methods to be identical, as each would execute a single escape burn to apoapsis, and correct inclination and periapsis in a second burn. The methods were designed with different flight plans to explore how each set of burns affected the resulting Delta-V to each asteroid. The comparison of the two provides insight into their relative efficiencies and inefficiencies for different orbital parameters.

4. Derivation: The 3 Burn Method

We now give the detailed derivation of the equations used to obtain the Delta-V for the two methods. As Burn 1 is common to both methods apart from the timing of the launch, we first derive Burn 1 in the context of the 3 Burn Method, and then modify it for the 2 Burn Method in Section 5.1.

4.1. 3 Burn Method: Burn 1

In both methods, the spacecraft starts in a circular parking orbit around the Earth in the plane of the ecliptic. As the spacecraft is orbiting Earth, the first burn occurs inside the Earth's gravity well. Thus, the spacecraft must first

escape the Earth's gravity to enter its own solar orbit. To achieve this, the spacecraft must reach escape velocity.

Escape velocity v_{esc} is reached when the kinetic energy of the orbiting spacecraft is equal to the gravitational potential energy at the spacecraft's current distance from the central body.

$$\frac{1}{2}mv_{esc}^2 = \frac{GM_{\oplus}m}{r} \tag{6}$$

In Eq. (6), m is the mass of the spacecraft (which is ultimately irrelevant to the energy comparison), G is Newton's Gravitational Constant, r is the orbital radius, and $M_{\oplus}$ is the mass of the Earth.

$$v_{esc}(r) = \sqrt{\frac{2GM_{\oplus}}{r}} = \sqrt{\frac{2\mu_{\oplus}}{r}} \tag{7}$$

Eq. (7) solves Eq. (6) for v_{esc} and establishes the standard gravitational parameter of the Earth.

For example, the escape velocity of a spacecraft in a 100 km orbit above the Earth's surface is 11.1 km s^{-1}. If the craft were to burn until its velocity equaled the escape velocity, then it would enter a parabolic orbit with respect to Earth such that as the spacecraft travelled far away from Earth, its relative velocity with Earth would tend to zero satisfying the time independent equivalence of potential and kinetic energy in Eq. (6). Although the craft's velocity would be zero relative to the Earth, the Earth has an orbital velocity around the Sun of $v_{\oplus}) = 29.8$ km s^{-1}. As the Earth's orbit is slightly eccentric ($e = 0.0167$), this value is not constant over the course of a year. We ignore this minor eccentricity for the purposes of this paper, and assume a perfectly circular orbit for the Earth. [3] Thus, after reaching escape velocity, when the spacecraft is far away from the Earth, the spacecraft would have a velocity around the Sun equal to the Earth's velocity.

[3] Another effect of this assumption is that there will be no preferential radial direction in the Sun-Earth system, so the Longitude of the Ascending Node can be ignored in all Delta-V calculations.

However, in the first burn, the spacecraft needs to not only escape from Earth, but also enter a transfer orbit with the same magnitude apoapsis as the asteroid it will intercept. Thus, it will accelerate beyond the escape velocity such that it travels faster than Earth and raises its solar orbit. This is referred to as the hyperbolic excess velocity v_∞. The hyperbolic excess velocity is the final speed of the spacecraft after it has travelled far away from the Earth's sphere of influence. This value is solved for using conservation of energy, where K_{bo} is the burn out kinetic energy of the spacecraft after it's escape burn, K_{esc} is the kinetic energy needed to escape the central body, C3 is the characteristic energy, or velocity at infinity v_∞ squared, and v_{bo} is the burn out velocity, the maximum velocity reached by the spacecraft during the burn.

$$K_{bo} - K_{esc} = \frac{1}{2}(\text{C3}) \tag{8}$$

$$\frac{1}{2}mv_{bo}^2 - \frac{1}{2}mv_{esc} = \frac{1}{2}m(\text{C3}) = \frac{1}{2}mv_\infty^2 \tag{9}$$

Solving for v_∞:

$$v_\infty = \sqrt{v_{bo}^2 - v_{esc}^2} \tag{10}$$

The burn out velocity v_{bo} will be the vector sum of the velocity of the spacecraft in its circular parking orbit v_p and the Delta-V of Burn 1 v_{M1}. By design, these vectors are collinear and thus add directly.

$$v_{bo} = v_p + v_{M1} \tag{11}$$

Once the spacecraft is far away from the Earth's sphere of influence, it is useful to switch reference frames from an Earth-centric reference frame to a solar reference frame. The Earth's reference frame orbits the Sun at the Earth's orbital velocity. Thus the spacecraft's orbital velocity around the Sun after Earth escape will be given by:

$$v_\odot = v_\infty + v_\oplus \tag{12}$$

The purpose of Burn 1 is to establish a transfer orbit apoapsis r_{Ap} equal to the apoapsis of the target asteroid. Using the geometry of an ellipse, the asteroid

apoapsis is given by:

$$r_{Ap} = a(1+e) \tag{13}$$

The periapsis of the transfer orbit r_{Pe} will be equal to the distance between the Earth and Sun $r_{\oplus}$. The semimajor axis of the transfer orbit a_t is then:

$$a_t = \frac{r_{Ap} + r_{Pe}}{2} = \frac{r_{Ap} + r_{\oplus}}{2} \tag{14}$$

Given this, the orbital velocity equation gives the target velocity around the Sun $v_{\odot}$ for such an orbit:

$$v(r) = \sqrt{\mu\left(\frac{2}{r} - \frac{1}{a}\right)} \qquad\qquad v_{\odot} = \sqrt{\mu\left(\frac{2}{r_{\oplus}} - \frac{1}{a_t}\right)} \tag{15}$$

From these equations, the value of v_{M1} can be determined as a function of the asteroid's semimajor axis and eccentricity.

Burn 1 should be performed when the Earth is 180 degrees around the Sun away from the apoapsis of the asteroid's orbit (see Figure 2) such that the transfer orbits apoapsis will have the same magnitude and ecliptic longitude as the asteroid's apoapsis.

Figure 2's "top-down" two-dimensional depiction of the orbits is misleading in that it that it fails to represent the orbital inclinations in three-dimensions. Thus, although the length and the (x, y) direction (ecliptic longitude) of the apoapsides may match, they are not necessarily aligned in (z) (ecliptic latitude), as depicted in Figure 3. This misalignment applies to any asteroid with both a nonzero inclination ($i \neq 0$) and an argument of periapsis equal to 0° or 180° degrees ($\omega \neq 0°, 180°$). For an asteroid with an orbital inclination of $i = 0$, the orbital plane is by definition the plane of the ecliptic, thus the vector pointing to the apoapsis has no (z) component, and the transfer orbit apoapsis will align perfectly. If the argument of the periapsis ω is either 0 degrees or 180 degrees, then the periapsis (and, by symmetry, the apoapsis) will coincide with the ascending/descending nodes. As the ascending and descending nodes are defined as the points where the asteroid orbit intersects the ecliptic plane (if inclination is zero ($i = 0$), then they are not defined, as the orbits are coplanar),

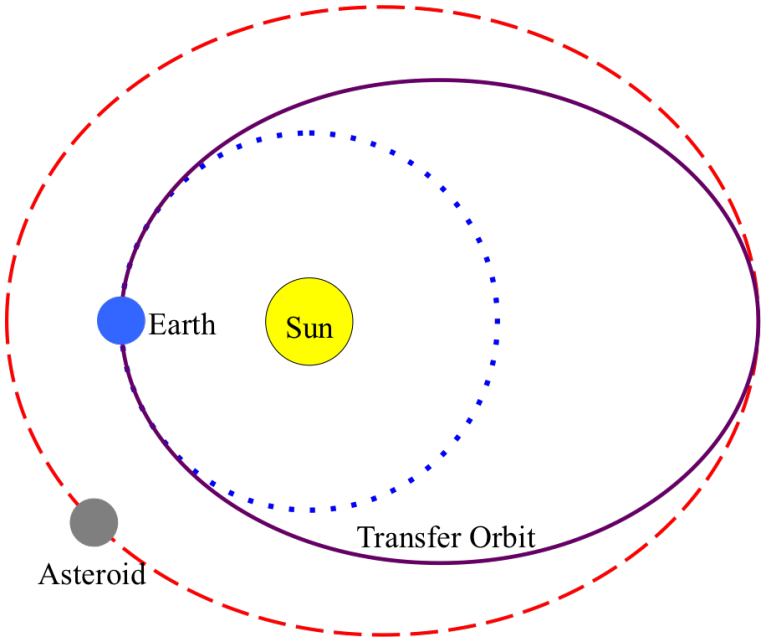

Figure 2: The orbits of the asteroid (red, dashed) , Earth (blue, dotted), and the spacecraft (purple, solid) after Burn 1, viewed from the ecliptic pole.

these also would have no (z) component. For a generalized orbit, this offset in (z) will be corrected in Burn 2.

4.2. 3 Burn Method: Burn 2

Burn 2 is performed during transfer and is designed to align the apoapsides of the two orbits. Pure inclination changes rely on changing the direction of the spacecraft's velocity vector while keeping its magnitude the same. This preserves the shape of the orbit, while changing the angle that it makes with the reference plane.

First, we calculate the ecliptic latitude of the apoapsis. By symmetry, this is simply the negative latitude of the periapsis. We start by defining the plane of the ecliptic to be the (x, y) plane. We then take the vector $(1, 0, 0)$ and define it as the vector pointing to the ascending node of the orbit $\vec{x}$.

$$\vec{x} = (1, 0, 0) \tag{16}$$

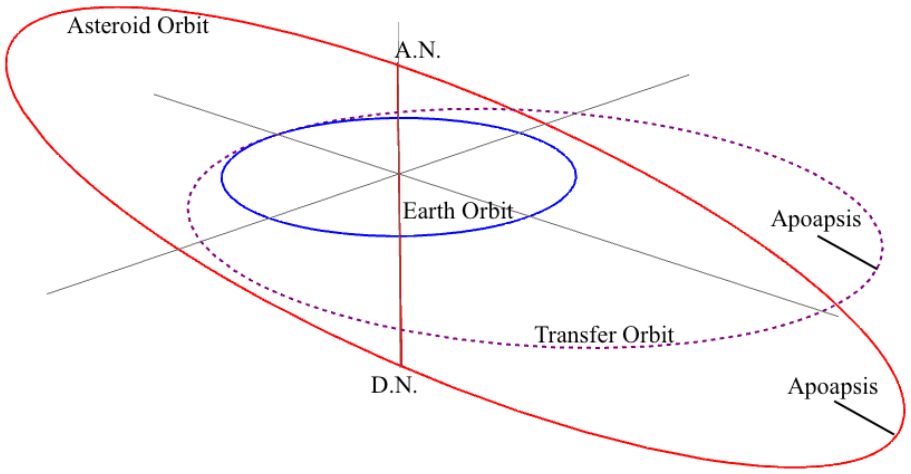

Figure 3: 3D diagram of the orbits of the Asteroid (solid red), Earth (solid blue), and the spacecraft (dotted purple) after Burn 1. The ascending and descending nodes of the asteroid's orbit are labeled by A.N. and D.N. respectively.

Next this vector is rotated by an angle ω around the z-axis equal to the argument of the periapsis.

$$\hat{R_z}(\omega)\vec{x} = (\cos(\omega), \sin(\omega), 0) \tag{17}$$

The resultant vector is then rotated about the x-axis by an angle i to generate the orbital inclination.

$$\hat{R_x}(i)(\cos(\omega), \sin(\omega), 0) = (\cos(\omega), \cos(i)\sin(\omega), \sin(i)\sin(\omega)) = \overrightarrow{Pe} \tag{18}$$

The resultant vector $\overrightarrow{Pe}$ points to the periapsis in cartesian coordinates. We are interested in the angle θ that this vector makes with the (x, y) plane, as this angle is the ecliptic latitude of the asteroid's periapsis. θ is complementary to the angle between the periapsis vector $\overrightarrow{Pe}$ and the z-axis $\vec{z}$. Taking the dot product of the periapsis vector $\overrightarrow{Pe}$ and the z-axis vector $\vec{z}$ gives:

$$\overrightarrow{Pe} \cdot \vec{z} = |\overrightarrow{Pe}||\vec{z}| \cos(90 - \theta) \tag{19}$$

$$\sin(\theta) = \sin(\omega)\sin(i) \tag{20}$$

Eq. (20) gives θ in terms of two known values, ω and i. (See Figure 4 for a depiction of this derivation).

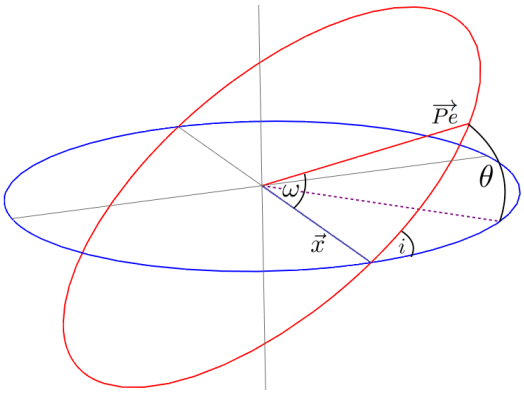

Figure 4: The blue vector is $\vec{x}$, the dashed purple vector is $\hat{R}_z(\omega)\vec{x}$, and the red vector is $\overrightarrow{Pe}$. The blue circle lies in the ecliptic plane, the red circle lies in the asteroid orbital plane. θ is the angle between the red vector and the blue circle.

Next we choose the location to perform the burn. By definition, the spacecraft and the central body (the Sun) must always be in the orbital plane. Thus, inclination changes will result in rotations about the axis formed by a line connecting the Sun and spacecraft. Since Burn 2 is designed to align the apoapsides of the transfer orbit and asteroid orbit, this burn should be performed at $\nu = 90°$. ν being the true anomaly, the angle between the periapsis and current orbital position. (Sec. 2)) Given $\nu = 90°$ and defining e_t as the eccentricity of the transfer orbit, we calculate the radius from the Sun at which Burn 2 is performed r_{M2}:

$$r_{M2} = r(\nu = 90°) = \frac{a(1-e^2)}{1 + e\cos(90°)} = a_t(1 - e_t^2) \tag{21}$$

Applying this result to the velocity equation gives the magnitude of the velocity of the spacecraft immediately before Burn 2 $v(r_{M2})$:

$$v(r_{M2}) = \sqrt{\mu\left(\frac{2}{r_{M2}} - \frac{1}{a_t}\right)} \tag{22}$$

Next we calculate the flight path angle ϕ, the angle between the spacecraft's velocity vector and the velocity vector of an object at the same radius moving in a circular orbit about the Sun (see Figure 6).

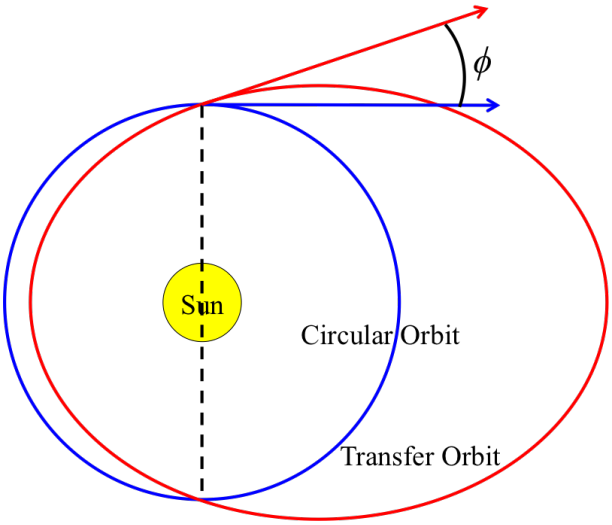

Figure 5: The blue vector is the tangential vector to the blue circular orbit, the red vector is the velocity vector for the red elliptical orbit. The angle between the two vectors is the flight path angle ϕ.

This flight path angle ϕ is important because in an inclination change of θ, θ is measured between the periapsis vector and the ecliptic plane, not along the direction of travel for the spacecraft. To correct for this, we derive the actual angular change Φ for Burn 2. Define $\vec{v_i}$ as the spacecraft's pre-burn velocity

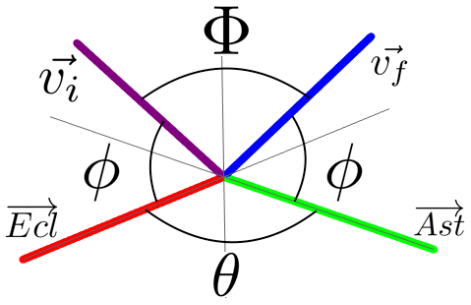

Figure 6: The vectors and angles used in calculating the inclination change angle Φ.

vector in the plane of the ecliptic, $\vec{v_f}$ as the spacecraft's post-burn velocity vector in the plane of the asteroid, $\overrightarrow{Ast}$ as a vector parallel to the asteroid's

apoapsis vector in the plane of the asteroid, and $\overrightarrow{Ecl} = (1, 0, 0)$ as a vector parallel to the spacecraft's apoapsis vector in the plane of the ecliptic. With these vector definitions we solve for Φ:

$$\vec{v_i} = \hat{R}_y(-\phi)\overrightarrow{Ecl} \qquad \vec{v_f} = \hat{R}_z(\theta)\vec{v_i} \tag{23}$$

By the definition of the dot product:

$$\vec{v_f} \cdot \vec{v_i} = \cos(\Phi) \tag{24}$$

Substituting in for $\vec{v_f}$ and $\vec{v_i}$:

$$[\hat{R}_y(-\phi)\overrightarrow{Ecl}] \cdot [\hat{R}_z(\theta)\vec{v_i}] = \cos(\Phi) \tag{25}$$

$$[\hat{R}_y(-\phi)(1, 0, 0)] \cdot [\hat{R}_z(\theta)\hat{R}_y(-\phi)(1, 0, 0)] = \cos(\Phi) \tag{26}$$

$$\cos(\Phi) = \cos(\theta)\cos^2(\phi) + \sin^2(\phi) \tag{27}$$

With the velocity change angle Φ defined, the law of cosines gives the Delta-V of Burn 2 (see Figure 7).

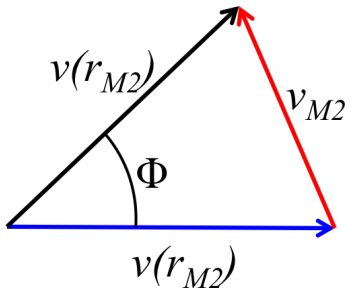

Figure 7: Triangle for the law of cosines consisting of Burn 2's Delta-V Vector (red) with the initial and final velocity vectors (blue and black), separated by the angle Φ.

$$v_{M2}^2 = v(r_{M2})^2 + v(r_{M2})^2 - 2v(r_{M2})v(r_{M2})\cos(\Phi) \tag{28}$$

$$v_{M2} = 2v(r_{M2})\sin\left(\frac{\Phi}{2}\right) \tag{29}$$

Figure 8 depicts the spacecraft, asteroid, and Earth orbits after Burn 2.

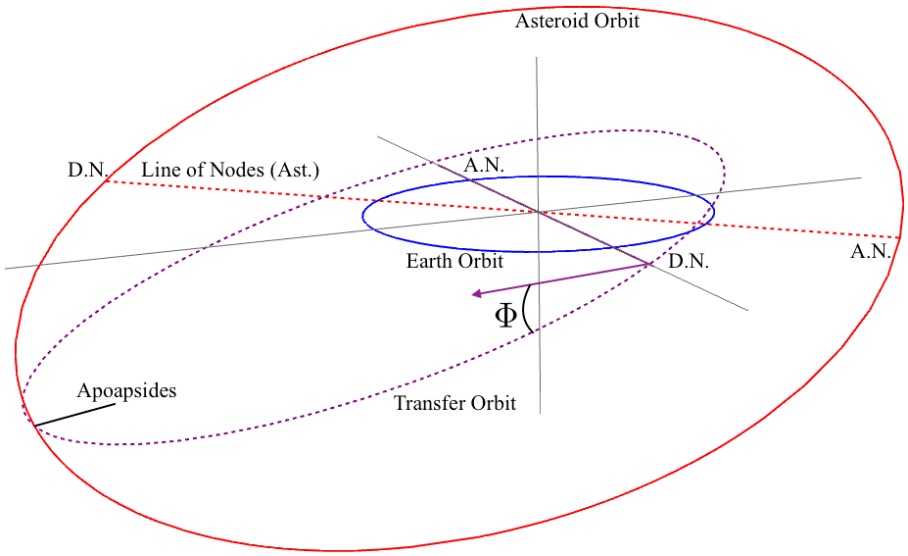

Figure 8: After Burn 2, the apoapsides of the asteroid and transfer orbits (red and dashed purple) coincide. The blue orbit is Earth's orbit for reference.

4.3. 3 Burn Method: Burn 3

The third and final burn of the 3 Burn Method is used to completely match orbits. This burn is performed at the shared apoapsis of the transfer and asteroid orbits. The burn both corrects any remaining inclination between the two orbital planes and matches their periapsides at the same time. These two parts of the orbital correction can be considered separately, and then combined later.

The periapsis correction is relatively simple. The velocity of the asteroid and spacecraft must be the same at apoapsis to share a periapsis. Using Eq. (4) the asteroid's velocity at apoapsis $v_{ast}(r_{Ap})$ is given by:

$$v_{ast}(r_{Ap}) = \sqrt{\mu\left(\frac{2}{r_{Ap}} - \frac{1}{a}\right)} \tag{30}$$

Similarly, the velocity of the spacecraft before the burn $v_{craft}(r_{Ap})$ is:

$$v_{craft}(r_{Ap}) = \sqrt{\mu\left(\frac{2}{r_{Ap}} - \frac{1}{a_t}\right)} \tag{31}$$

where a_t is the semimajor axis of the transfer orbit defined in Burn 1 and calculated in Eq. (14).

Calculating the remaining inclination change is more difficult. As the apoapsides and the Sun lie in both orbital planes as a result of Burn 2, they form the current axis of inclination of the spacecraft relative to the asteroid. Thus, the apoapsis and periapsis are the ascending/descending nodes. This is by design, so that the periapsis correction and remaining inclination angle ψ can be corrected with the same burn. ψ is calculated by constructing normal vectors to the orbital planes. To find these normal vectors, we choose two vectors in each plane and take their cross product to generate a normal vector.

For the Asteroid's orbital plane, we first choose the periapsis vector $\overrightarrow{Pe}$ as defined in Burn 2. To select the second vector in the asteroid's orbital plane, we recall that in our initial determination of the periapsis vector's position (see Section 4.2), we applied rotation operators to $\vec{x} = (1, 0, 0)$. In doing so, $\vec{x}$ was defined as the ascending node of the asteroid's orbit relative to the ecliptic. Thus, $\vec{x}$ lies in the orbital plane and can be crossed with $\overrightarrow{Pe}$ to find a normal vector to the plane.

$$\vec{x} \times \overrightarrow{Pe} = (1, 0, 0) \times (\cos(\omega), \cos(i)\sin(\omega), \sin(i)\sin(\omega)) \tag{32}$$

$$\overrightarrow{n_{ast}} = (0, -\sin(i)\sin(\omega), \cos(i)sin(\omega)) \tag{33}$$

Normalizing the normal vector in preparation for a dot product gives:

$$\overrightarrow{N_{ast}} = (0, -\sin(i), \cos(i)) \tag{34}$$

The transfer orbital plane also contains the periapsis vector, but a second vector must be identified to find the normal vector. A good choice is the vector leading to the position at which Burn 2 was performed. Recall that this burn occurred in the ecliptic (x, y) plane and was performed at $\nu = 90°$. To reconstruct this vector, we first project $\overrightarrow{Pe}$ onto the (x, y) plane, then rotate it $-90°$ about the z-axis.

$$\overrightarrow{M2} = \hat{R}_z(-90°)[\overrightarrow{Pe} \cdot (1, 1, 0)] = (\cos(i)\sin(\omega), -\cos(\omega), 0) \tag{35}$$

The normal vector is given by the cross product:

$$\overrightarrow{M2} \times \overrightarrow{Pe} = (\cos(i)\sin(\omega), -\cos(\omega), 0) \times (\cos(\omega), \cos(i)\sin(\omega), \sin(i)\sin(\omega)) \tag{36}$$

$$\overrightarrow{n_{craft}} = (-\cos(\omega)\sin(i)\sin(\omega), -\cos(i)\sin(i)\sin^2(\omega), \cos^2(\omega) + \cos^2(i)\sin^2(\omega)) \tag{37}$$

Normalizing the normal vector in preparation for a dot product gives:

$$\overrightarrow{N_{craft}} = \left(\frac{-\cos(\omega)\sin(i)\sin(\omega)}{\sqrt{\cos^2(\omega) + \cos^2(i)\sin^2(\omega)}}, \frac{-\cos(i)\sin(i)\sin^2(\omega)}{\sqrt{\cos^2(\omega) + \cos^2(i)\sin^2(\omega)}}, \sqrt{\cos^2(\omega) + \cos^2(i)\sin^2(\omega))} \right) \tag{38}$$

The cosine of the angle between the orbital planes ψ is given by the dot product of the two normal vectors.

$$\overrightarrow{N_{craft}} \cdot \overrightarrow{N_{ast}} = \cos(\psi) \tag{39}$$

$$\cos(\psi) = \frac{\cos(i)}{\sqrt{\cos^2(\omega) + \cos^2(i)\sin^2(\omega)}} \tag{40}$$

Having solved for ψ, the Delta-V for Burn 3 is given by the law of cosines applied to the two velocity vectors and the angle between them:

$$v_{M3}^2 = v_{ast}^2 + v_{craft}^2 - 2v_{ast}v_{craft}\cos(\psi) \tag{41}$$

$$v_{M3} = \sqrt{v_{ast}^2 + v_{craft}^2 - 2v_{ast}v_{craft}\cos(\psi)} \tag{42}$$

The resulting orbit from Burn 3 is shown below.

4.4. The 3 Burn Method: Delta-V

The final Delta-V (ΔV) for the 3 Burn Method is simply the sum of the Delta-V's for each burn.

$$\Delta V = v_{M1} + v_{M2} + v_{M3} \tag{43}$$

It should be noted that this Delta-V only reflects the outbound journey to an asteroid.

In the 3 Burn Method, rendezvous with the asteroid occurs at the asteroid's

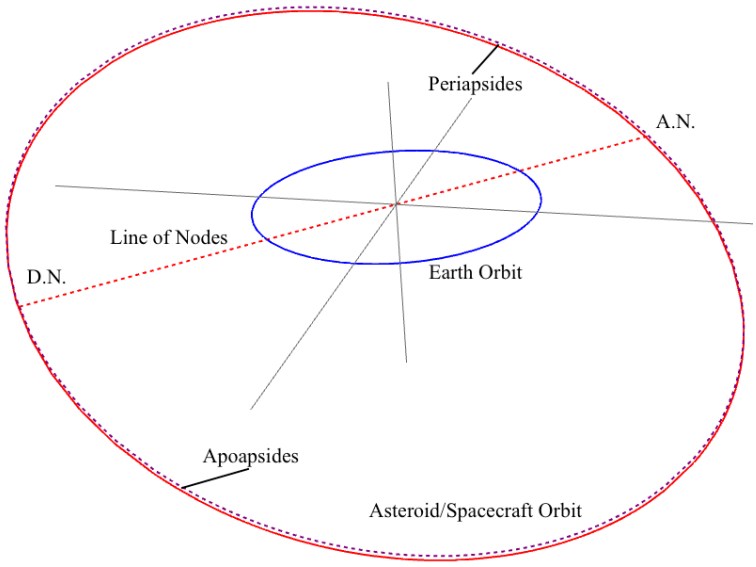

Figure 9: After Burn 3, the asteroid and spacecraft orbits (red and dashed purple) are fully aligned. The blue orbit is Earth's orbit for reference.

apoapsis, after a single half transfer orbit.

In order for this rendezvous to occur, Burn 1 must be executed at the proper time to ensure that the asteroid and spacecraft meet up at the apoapsis. This launch window is specific to each individual asteroid, and is reliant upon the proper alignment of the asteroid and the Earth[4].

5. Derivation: The 2 Burn Method

5.1. The 2 Burn Method: Burn 1 Modifications

Burn 1 is nearly identical to Burn 1 of the 3 Burn Method. The only difference is that it it designed to reach a different transfer apoapsis height a_t at a different ecliptic longitude. The burn is designed to cause the spacecraft to intercept the orbital path of the asteroid without any plane/inclination changes.

[4]See the Future Directions section for a possible investigation into this and its effect on mission Delta-V

The only points in the asteroid's orbit that lies in the ecliptic plane are the ascending and descending nodes. Unlike the singular apoapsis target, this gives a choice of two targets. It is preferable to choose the higher of the two nodes, as this will decrease the velocity needed to match orbits in the second burn (see later discussion on efficiency for a full explanation). To find the heights of the two nodes, we use Kepler's orbital radius equation.

$$r(\nu) = \frac{a(1-e^2)}{1+e\cos(\nu)} \tag{44}$$

The true anomalies ν of the nodes are given by the definition of the argument of the periapsis ω. Thus, the nodes are located at $\nu = -\omega$ and $\nu = 180° - \omega$. Using the Kepler equation, the higher of the two can be determined. Let the height and true anomaly of the higher node be denoted by r_1 and ν_1 respectively.

With these values and the new target established, the following equations (14, 10+12+15, 11) are applied from the first method.

$$a_t = \frac{r_1 + r_\oplus}{2} \qquad \sqrt{v_{bo}^2 - v_{esc}^2} + v_\oplus = \sqrt{\mu\left(\frac{2}{r_\oplus} - \frac{1}{a_t}\right)} \qquad v_{bo} = v_p + v_{M1} \tag{45}$$

Just as before, solving these equations for v_{M1} yields the Delta-V of the first burn. Figures 10 and 11 illustrate Burn 1.

5.2. 2 Burn Method: Burn 2

Burn 2 of the 2 Burn Method is most similar to The 3 Burn Method's Burn 3, in that it functions by aligning both orbital velocity and orbital inclination. Thus, the initial and final velocity vector directions and magnitudes must be calculated. The velocity magnitudes are calculated using the Keplerian velocity equation, where r_n is the radius of the ascending/descending node at which Burn 2 is performed.

$$v_{craft} = \sqrt{\mu\left(\frac{2}{r_n} - \frac{1}{a_t}\right)} \tag{46}$$

$$v_{ast} = \sqrt{\mu\left(\frac{2}{r_n} - \frac{1}{a}\right)} \tag{47}$$

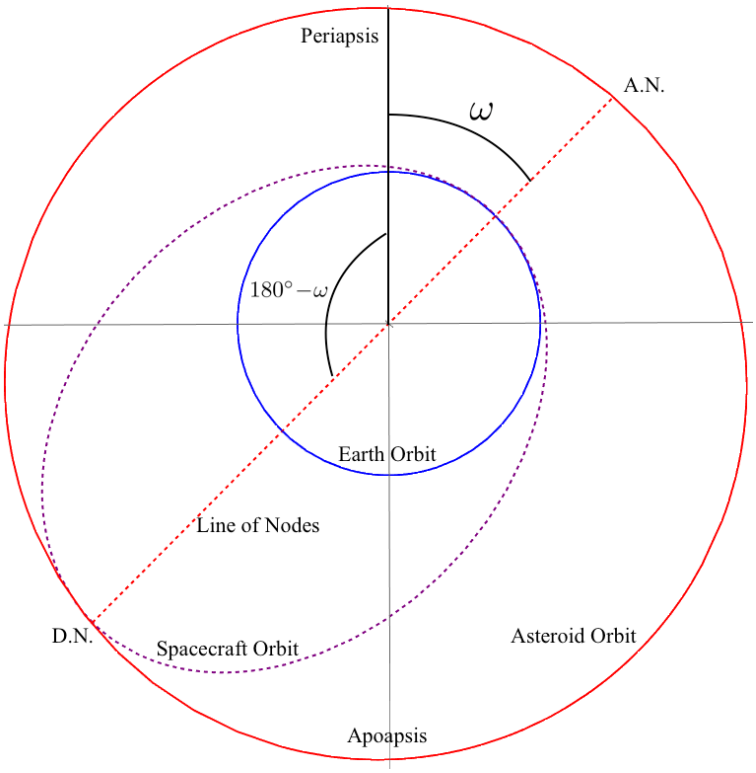

Figure 10: Top view of the orbits of the Asteroid (red), Earth (blue), and the Spacecraft (dashed purple) after Burn 1.

Next we calculate the directions of the velocity vectors in 3D space. Up until this point, we have used a coordinate system where the ecliptic plane is defined as the (x, y) plane. However, we now will define the (x, y) plane as the plane of the asteroid's orbit. In this new coordinate system, the asteroid's orbit can be written as a simple ellipse.

$$\frac{(x+c)^2}{a^2} + \frac{y^2}{b^2} = 1 \tag{48}$$

In this equation, a is the semimajor axis, b is the semiminor axis, and c is the distance between the center of the ellipse and the foci of the ellipse. The before mentioned variables are related by the following equations:

$$c = ae \qquad a^2 = b^2 + c^2 \tag{49}$$

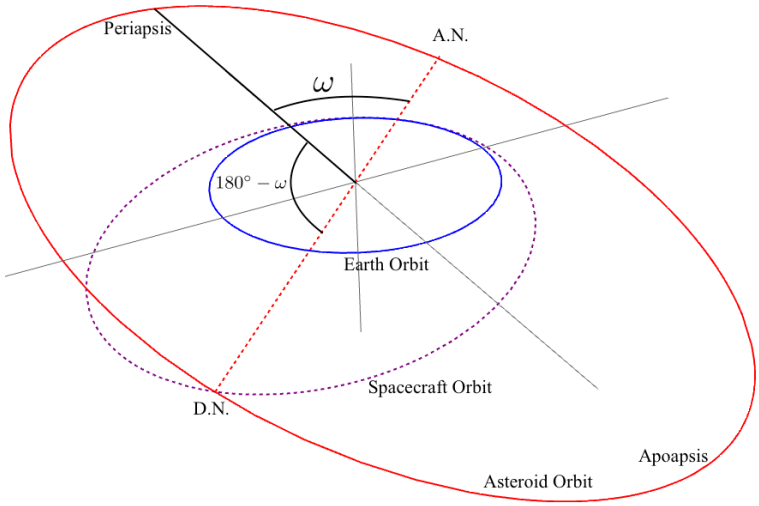

Figure 11: 3D view of the orbits of the Asteroid (red), Earth (blue), and the Spacecraft (dashed purple) after Burn 1.

As a and e are givens, b and c can be calculated for any asteroid orbit. By using the offset of c, the Sun (one focus) is returned to the origin. The velocity vector in an elliptical orbit is always tangent to its point of origin on the ellipse. To find a tangent vector to an ellipse, we first take the gradient of the equation of the ellipse to find the normal vectors at each point on the ellipse.

$$\nabla\left(\frac{(x+c)^2}{a^2}+\frac{y^2}{b^2}\right)=\left(\frac{2(x+c)}{a^2},\frac{2y}{b^2}\right) \tag{50}$$

Tangent vectors are always orthogonal to normal vectors, thus the tangent vectors to an ellipse are given by:

$$\left(\frac{-2y}{b^2},\frac{2(x+c)}{a^2}\right) \tag{51}$$

As we only care about direction, this simplifies to:

$$\left(\frac{-y}{b^2},\frac{x+c}{a^2}\right) \tag{52}$$

Converting this equation into cylindrical coordinates yields:

$$x=r(\nu)\cos(\nu) \qquad\qquad y=r(\nu)\sin(\nu) \tag{53}$$

$$\left(\frac{-r(\nu)\sin(\nu)}{b^2}, \frac{r(\nu)\cos(\nu)+c}{a^2}\right) \tag{54}$$

Since this vector represents the velocity vector of an asteroid in 3D space, the vector is given by:

$$\overrightarrow{v_{ast}} = \left(\frac{-r(\nu_1)\sin(\nu_1)}{b^2}, \frac{r(\nu_1)\cos(\nu_1)+c}{a^2}, 0\right) \tag{55}$$

The velocity vector for the spacecraft is significantly easier to find. Since the spacecraft intersects the asteroid's orbit at the transfer orbit apoapsis, the spacecraft's flight path angle is 0. Thus, its velocity vector points orthogonally to the vector pointed towards the spacecraft from the central body. The velocity vector of the craft is thus tangent to a circle, and is given by:

$$(-\sin(\nu_1), \cos(\nu_1)) \tag{56}$$

Using the new asteroid based coordinate system, the craft's velocity vector is inclined relative to the (x, y) plane. Since the craft is at the ascending node, this inclination is exactly i. Rotating the vector by i about the radial axis produces the 3D craft velocity vector.

$$\overrightarrow{v_{craft}} = \hat{R_r}(i)(-\sin(\nu_1), \cos(\nu_1), 0) = (-\sin(\nu_1)\cos(i), \cos(\nu_1)\cos(i), \sin(i)) \tag{57}$$

Taking the dot product of the two normalized vectors produces the angle between them.

$$\frac{\overrightarrow{v_{craft}}}{|\overrightarrow{v_{craft}}|} \cdot \frac{\overrightarrow{v_{ast}}}{|\overrightarrow{v_{ast}}|} = \cos(\Psi) \tag{58}$$

With both vector magnitudes and the angle known, the Delta-V of Burn 2 v_{M2} is given by the law of cosines.

$$v_{M2} = \sqrt{v_{craft}^2 + v_{ast}^2 - 2v_{craft}v_{ast}\cos(\Psi)} \tag{59}$$

The execution of this burn once again results in orbital alignment and rendezvous.

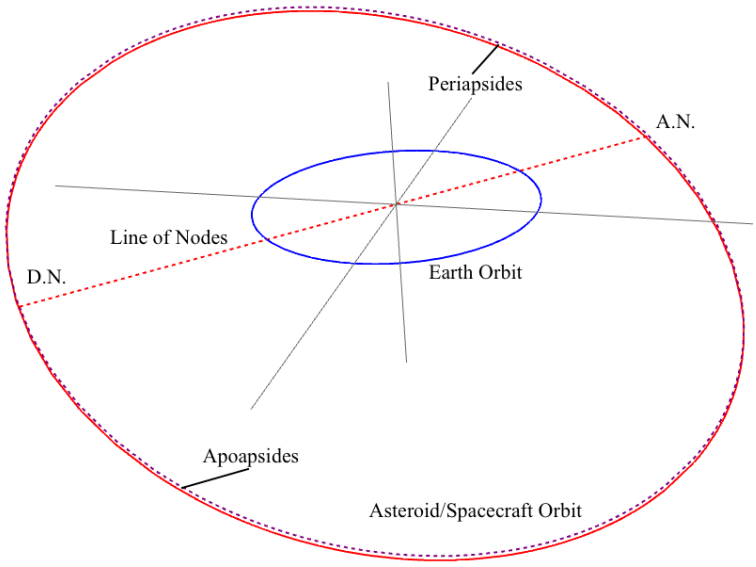

Figure 12: After Burn 2, the asteroid and spacecraft orbits (red and dashed purple) are fully aligned. The blue orbit is Earth's orbit for reference.

5.3. The 2 Burn Method: Delta-V

The final Delta-V (ΔV) for the 2 Burn Method is the sum of the Delta-V of each burn.

$$\Delta V = v_{M1} + v_{M2} \tag{60}$$

As before, this expression represents the Delta-V necessary to rendezvous with an asteroid, not the Delta-V for the round trip back to Earth.

This method also requires a proper alignment of the asteroid and Earth to execute a proper rendezvous such that the asteroid and spacecraft arrive at the chosen ascending/descending node at the same time.

6. Data Analysis

6.1. Input Data

The chosen dataset for the orbital analysis is the Minor Planet Center Orbit Database (MPCORB) accessed on October 3, 2016.[5] This dataset is the product of individual observers' data on solar system objects and contains data on over 700,000 asteroid orbits, including both the numbered objects and provisional objects. Both the numbered and provisional objects were used in this study. The datafile is an ASCII based text file (see Figure 13). The datafile uses blank entries for missing data points (as opposed to "–", "NaN","n/a", etc). This proved troublesome when reading in the dataset using the Python function "numpy.genfromtxt".[6] Using "Find and Replace" commands in a text editor, blanks were identified and replaced with the string "FIX_" to simplify the import process.

The data read in were: object designation (Des'n), argument of periapsis (Peri.), inclination (Incl.), eccentricity (e), and semimajor axis (a).

6.2. Code

Both orbital rendezvous methods were implemented in IPython Notebook (Python 2.7.10). The code consists of three parts, the 3 Burn Method Calculations (Appendix A), the 2 Burn Method Calculations (Appendix B), and the Data Analysis code (Appendix C) that creates the final output data file.

The code was run on on a Late 2011 15" MacBook Pro (MacBookPro8,2) running MacOS 10.12.1 and applied to the dataset, producing a set of two Delta-V values (one for each method) for each object for the dataset. While calculating the Delta-V for all 700,000 objects, the code ran for around 10 minutes for each burn method and used no more than 2 GB of RAM.

A starting Earth parking orbit height of 100 km (LEO) was used throughout. A comparison was then applied to the dataset to determine the better optimized

[5]This dataset is available and updated daily at http://www.minorplanetcenter.org/iau/MPCORB/MPCORB.DAT

[6]More sophisticated read-in commands can be used to bypass this issue.

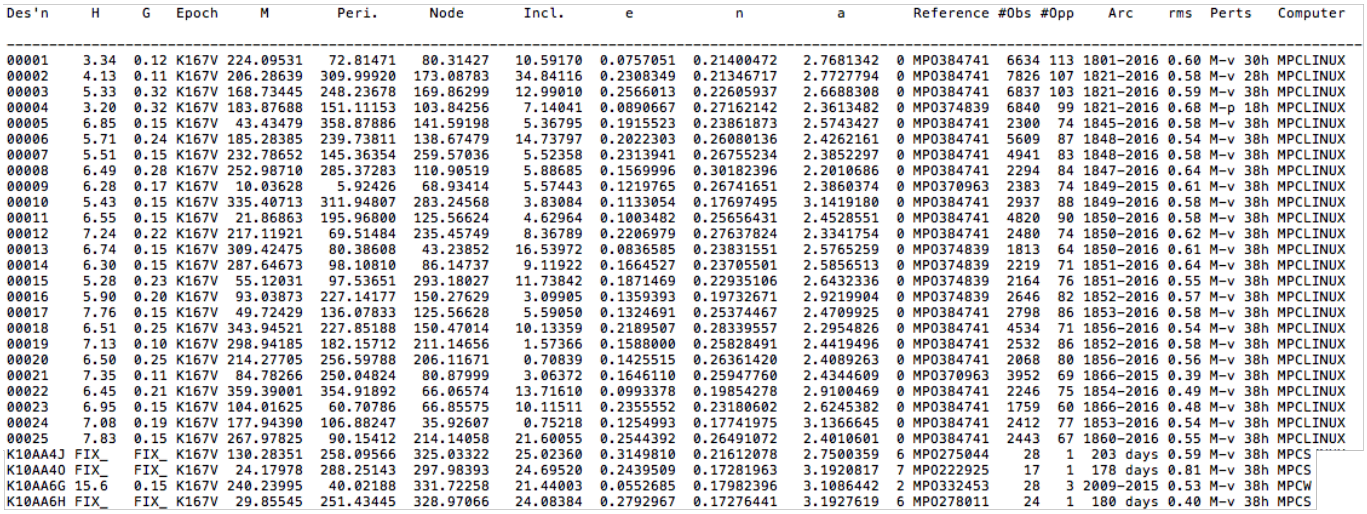

Des'n	H	G	Epoch	M	Peri.	Node	Incl.	e	n	a	Reference	#Obs	#Opp	Arc	rms	Perts	Computer
00001	3.34	0.12	K167V	224.09531	72.81471	80.31427	10.59170	0.0757051	0.21400472	2.7681342	0 MPO384741	6634	113	1801-2016	0.60	M-v 30h	MPCLINUX
00002	4.13	0.11	K167V	206.28639	309.99920	173.08783	34.84116	0.2308349	0.21346717	2.7727794	0 MPO384741	7826	107	1821-2016	0.58	M-v 28h	MPCLINUX
00003	5.33	0.32	K167V	168.73445	248.23678	169.86299	12.99010	0.2566013	0.22605937	2.6688308	0 MPO384741	6837	103	1821-2016	0.59	M-v 38h	MPCLINUX
00004	3.20	0.32	K167V	183.87688	151.11153	103.84256	7.14041	0.0890667	0.27162142	2.3613482	0 MPO374839	6840	99	1821-2016	0.68	M-p 18h	MPCLINUX
00005	6.85	0.15	K167V	43.43479	358.87886	141.59198	5.36795	0.1915523	0.23861873	2.5743427	0 MPO384741	2300	74	1845-2016	0.58	M-v 38h	MPCLINUX
00006	5.71	0.24	K167V	185.28385	239.73811	138.67479	14.73797	0.2022303	0.26080136	2.4262161	0 MPO384741	5609	87	1848-2016	0.54	M-v 38h	MPCLINUX
00007	5.51	0.15	K167V	232.78652	145.36354	259.57036	5.52358	0.2313941	0.26755234	2.3852297	0 MPO384741	4941	83	1848-2016	0.58	M-v 38h	MPCLINUX
00008	6.49	0.28	K167V	252.98710	285.37283	110.90519	5.88685	0.1569996	0.30182396	2.2010686	0 MPO384741	2294	84	1847-2016	0.64	M-v 38h	MPCLINUX
00009	6.28	0.17	K167V	10.03628	5.92426	68.93414	5.57443	0.1219765	0.26741651	2.3860374	0 MPO370963	2383	74	1849-2015	0.61	M-v 38h	MPCLINUX
00010	5.43	0.15	K167V	335.40713	311.94807	283.24568	3.83084	0.1133054	0.17697495	3.1419180	0 MPO384741	2937	88	1849-2016	0.58	M-v 38h	MPCLINUX
00011	6.55	0.15	K167V	21.86863	195.96800	125.56624	4.62964	0.1003482	0.25656431	2.4528551	0 MPO384741	4820	90	1850-2016	0.58	M-v 38h	MPCLINUX
00012	7.24	0.22	K167V	217.11921	69.51484	235.45749	8.36789	0.2206979	0.27637824	2.3341754	0 MPO384741	2480	74	1850-2016	0.62	M-v 38h	MPCLINUX
00013	6.74	0.15	K167V	309.42475	80.38608	43.23852	16.53972	0.0836585	0.23831551	2.5765259	0 MPO374839	1813	64	1850-2016	0.61	M-v 38h	MPCLINUX
00014	6.30	0.15	K167V	287.64673	98.10810	86.14737	9.11922	0.1664527	0.23705501	2.5856513	0 MPO374839	2219	71	1851-2016	0.64	M-v 38h	MPCLINUX
00015	5.28	0.23	K167V	55.12031	97.53651	293.18027	11.73842	0.1871469	0.22935106	2.6432336	0 MPO374839	2164	76	1851-2016	0.55	M-v 38h	MPCLINUX
00016	5.90	0.20	K167V	93.03873	227.14177	150.27629	3.09905	0.1359393	0.19732671	2.9219904	0 MPO374839	2646	82	1852-2016	0.57	M-v 38h	MPCLINUX
00017	7.76	0.15	K167V	49.72429	136.07833	125.56628	5.59050	0.1324691	0.25374467	2.4709925	0 MPO384741	2798	86	1853-2016	0.58	M-v 38h	MPCLINUX
00018	6.51	0.25	K167V	343.94521	227.85188	150.47014	10.13359	0.2189507	0.28339557	2.2954826	0 MPO384741	4534	71	1856-2016	0.54	M-v 38h	MPCLINUX
00019	7.13	0.10	K167V	298.94185	182.15712	211.14656	1.57366	0.1588000	0.25828491	2.4419496	0 MPO384741	2532	86	1852-2016	0.58	M-v 38h	MPCLINUX
00020	6.50	0.25	K167V	214.27705	256.59788	206.11671	0.70839	0.1425515	0.26361420	2.4089263	0 MPO384741	2068	80	1856-2016	0.56	M-v 38h	MPCLINUX
00021	7.35	0.11	K167V	84.78266	250.04824	80.87999	3.06372	0.1646110	0.25947760	2.4344609	0 MPO370963	3952	69	1866-2015	0.39	M-v 38h	MPCLINUX
00022	6.45	0.21	K167V	359.39001	354.91892	66.06574	13.71610	0.0993378	0.19854278	2.9100469	0 MPO384741	2246	75	1854-2016	0.49	M-v 38h	MPCLINUX
00023	6.95	0.15	K167V	104.01625	60.70786	66.85575	10.11511	0.2355552	0.23180602	2.6245382	0 MPO384741	1759	60	1866-2016	0.48	M-v 38h	MPCLINUX
00024	7.08	0.19	K167V	177.94390	106.88247	35.92607	0.75218	0.1254993	0.17741975	3.1366645	0 MPO384741	2412	77	1853-2016	0.54	M-v 38h	MPCLINUX
00025	7.83	0.15	K167V	267.97825	90.15412	214.14058	21.60055	0.2544392	0.26491072	2.4010601	0 MPO384741	2443	67	1860-2016	0.55	M-v 38h	MPCLINUX
K10AA4J	FIX_	FIX_	K167V	130.28351	258.09566	325.03322	25.02360	0.3149810	0.21612078	2.7500359	6 MPO275044	28	1	203 days	0.59	M-v 38h	MPCS
K10AA4O	FIX_	FIX_	K167V	24.17978	288.25143	297.98393	24.69520	0.2439509	0.17281963	3.1920817	7 MPO222925	17	1	178 days	0.81	M-v 38h	MPCS
K10AA6G	15.6	0.15	K167V	240.23995	40.02188	331.72258	21.44003	0.0552685	0.17982396	3.1086442	2 MPO332453	28	3	2009-2015	0.53	M-v 38h	MPCW
K10AA6H	FIX_	FIX_	K167V	29.85545	251.43445	328.97066	24.08384	0.2792967	0.17276441	3.1927619	6 MPO278011	24	1	180 days	0.40	M-v 38h	MPCS

Figure 13: The first few rows and columns of data from MPCORB.DAT. The last few rows demonstrate the "FIX_" replacement.

Delta-V and each entry was tagged with the method that calculated the lower Delta-V[7]. Additional code was used to combine the output datasets from each method and to analyze the final dataset and produce plots as needed.

6.3. Output Dataset

The resulting output dataset (see Figure 14) writes out for each object: object designation (Des'n), argument of periapsis (Peri.), inclination (Incl.), eccentricity (e), semimajor axis (a), Delta-V for the 3 Burn Method (DV1), Delta-V for the 2 Burn Method (DV2), the lower Delta-V value (DV_BEST), and the number of the Method that produced the lower Delta-V value (Method).

6.4. Comparison of Methods

The two different rendezvous methods provide remarkably similar results when applied to the dataset.

[7]In the output file, "1" Corresponds to the 3 Burn Method, "2" corresponds to the 2 Burn Method

```
Des'n|  Peri. |  Incl. |    e    |    a    |   DV1  |   DV2  |DV_BEST |Method
00001 72.81471 10.59170 0.0757100 2.7681300 13809.87 10569.54 10569.54 2
00002 309.99920 34.84116 0.2308300 2.7727800 22294.73 14740.82 14740.82 2
00003 248.23678 12.99010 0.2566000 2.6688300 13589.72 11797.35 11797.35 2
00004 151.11153 7.14041 0.0890700 2.3613500 10432.06 9168.85 9168.85 2
00005 358.87886 5.36795 0.1915500 2.5743400 8803.53 8760.04 8760.04 2
00006 239.73811 14.73797 0.2022300 2.4262200 14055.30 11202.43 11202.43 2
00007 145.36354 5.52358 0.2313900 2.3852300 9447.09 9213.00 9213.00 2
00008 285.37283 5.88685 0.1570000 2.2010700 10333.68 9665.15 9665.15 2
00009 5.92426 5.57443 0.1219800 2.3860400 9005.34 8770.81 8770.81 2
00010 311.94807 3.83084 0.1133100 3.1419200 11067.86 10280.70 10280.70 2
00011 195.96800 4.62964 0.1003500 2.4528600 9448.56 8963.61 8963.61 2
00012 69.51484 8.36789 0.2207000 2.3341800 11282.45 10654.35 10654.35 2
00013 80.38608 16.53972 0.0836600 2.5765300 16083.43 11414.97 11414.97 2
00014 98.10810 9.11922 0.1664500 2.5856500 12517.37 10740.54 10740.54 2
00015 97.53651 11.73842 0.1871500 2.6432300 13608.00 11310.10 11310.10 2
00016 227.14177 3.09905 0.1359400 2.9219900 10399.65 9975.30 9975.30 2
00017 136.07833 5.59050 0.1324700 2.4709900 10411.66 9371.35 9371.35 2
00018 227.85188 10.13359 0.2189500 2.2954800 11443.33 10093.99 10093.99 2
00019 182.15712 1.57366 0.1588000 2.4419500 8465.38 8442.37 8442.37 2
00020 256.59788 0.70839 0.1425500 2.4089300 8720.87 9624.00 8720.87 1
00021 250.04824 3.06372 0.1646100 2.4344600 9612.61 9816.35 9612.61 1
00022 354.91892 13.71610 0.0993400 2.9100500 11141.34 10645.87 10645.87 2
00023 60.70786 10.11511 0.2355600 2.6245400 12293.54 10990.82 10990.82 2
00024 106.88247 0.75218 0.1255000 3.1366600 10080.37 10534.51 10080.37 1
00025 90.15412 21.60055 0.2544400 2.4010600 16930.74 13773.26 13773.26 2
```

Figure 14: The first few rows of data from the output file. The heading was added manually for display purposes, and is not included in the raw output file to increase readability by computers.

Figure 15 shows the Delta-V distributions for each method. Clearly, the 3 Burn Method is more efficient for some entires in the 8-9 km s^{-1} range, as the Best Method distribution is greater than the plot for the 2 Burn Method. After $\sim$13 km s^{-1}, the 2 Burn Method and Best Method distributions converge demonstrating that the 3 Burn Method is comparatively inefficient for these objects. These objects (especially those with a Delta-V between 13-15 km s^{-1}) tend to have an argument of periapsis ω between $30° - 150°$ or $220° - 330°$. These arguments of the periapsis result in Burn 2 of the 3 Burn Method causing the majority of the inclination change. This is relatively costly in Delta-V, as demonstrated in the later discussion of the relative efficiency of each method's burns.

The 2 Burn Method showed on average, an 8% decrease in Delta-V relative to the 3 Burn Method. However, the 3 Burn Method still outperformed the 2 Burn Method in 14.6% of the dataset objects. This 8% decrease in Delta-V

may appear minor, but finding the minimal Delta-V path for a mission is critical to the budget and capacity of a mission as previously discussed regarding the rocket equation. Therefore, we define an efficient burn or method as one that minimizes Delta-V.

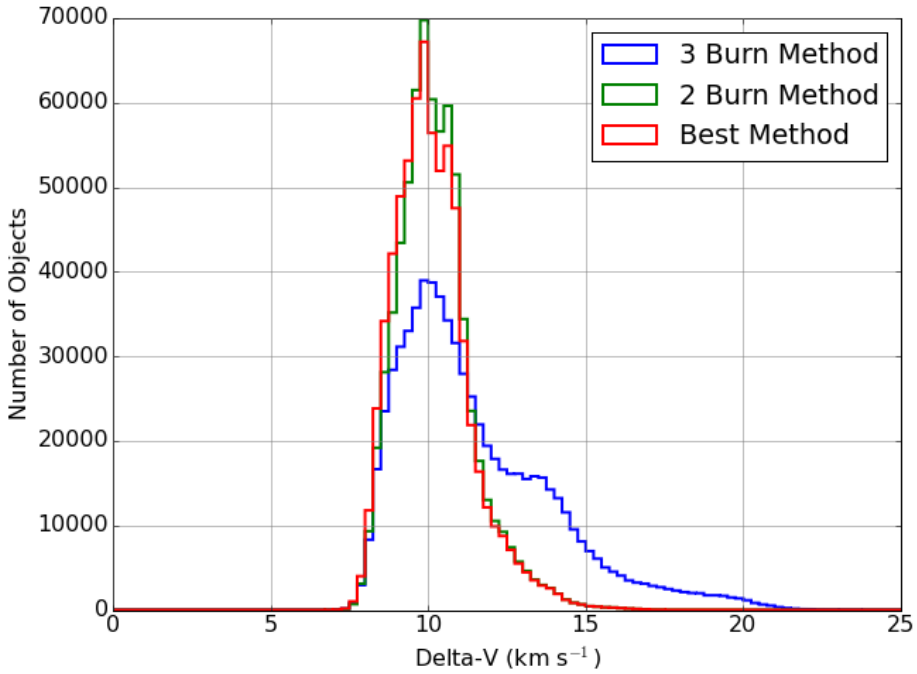

Figure 15: Distributions of Main Belt asteroid (non-Main Belt objects have been filtered out) Delta-V in the dataset for the 3 Burn Method (blue), the 2 Burn Method (green) and the best Method for each datapoint (red)

To investigate which objects are preferred by each method, Figure 16 plots the inclination and semimajor axis of the asteroids best reached by each of the two methods separately in a heat map. Figure 16 demonstrates that the 3 Burn Method tends to be preferred only for orbits with low orbital inclination. This makes sense, as the 3 Burn Method is most efficient in its first and third burns. The first burn is efficient because it sets the apoapsis of the orbit while at the periapsis, making maximum use of the Oberth Effect with respect to both Earth and the Sun. Since a rocket is a momentum engine, the acceleration it generates

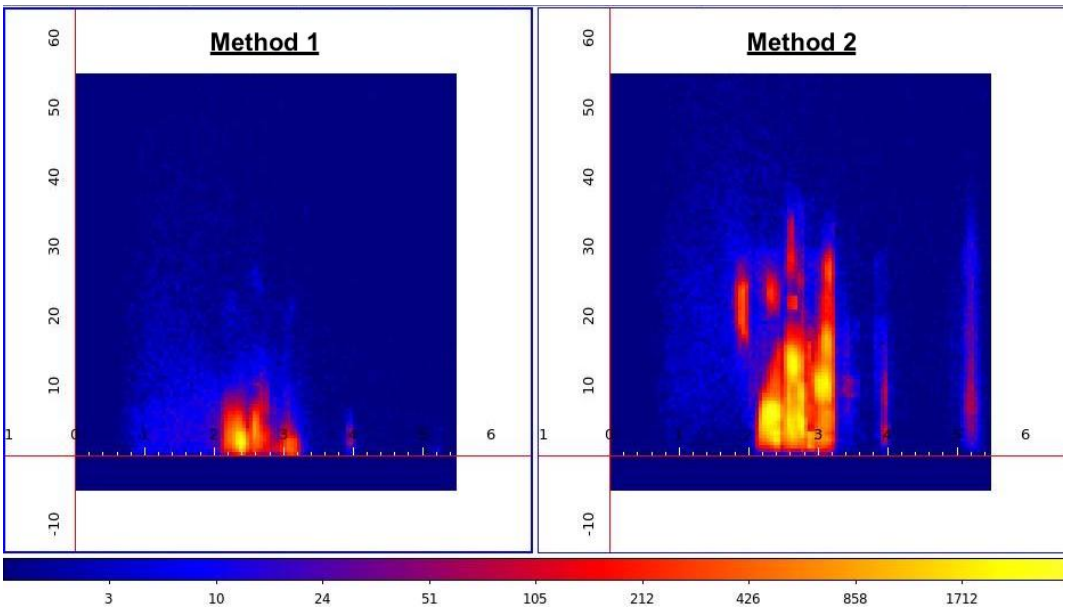

Figure 16: Asteroid inclination plotted against semimajor axis. The left plots shows the density of asteroids best reached by the 3 Burn Method. The right plot shows the density of asteroids best reached by the 2 Burn Method.

is independent of the rocket's current orbital speed. Because kinetic energy is given by $K = (1/2)mv^2$, accelerating linearly at a high velocity results in a greater kinetic energy increase than at lower velocity. This is known as the Oberth Effect, and it explains why the periapsis is the best location from which to raise the apoapsis [1].

Burn 3 is efficient for three reasons.

1. Burn 3 raises the periapsis at the apoapsis. Ignoring the simultaneous inclination change, this is efficient because all of the rocket's Delta-V is added directly to the current velocity vector. Burns at an angle to the velocity vector are inherently inefficient, as the magnitude of the resulting vector is less than or equal to the sum of magnitudes of the original velocity vector and the burn vector.
2. Orbital inclination is adjusted at the apoapsis. This is important, because

an inclination change involves changing the direction of the velocity vector. Thus, it is most efficient to do this when the velocity is minimal. For example, if the magnitude of the velocity is 500 m s^{-1}, then a 1000 m s^{-1} burn would be necessary to reverse the orbit direction (the most extreme inclination change possible). However, if the velocity is only 50 m s^{-1}, then a 100 m s^{-1} burn will suffice. This applies to Burn 3 because the apoapsis is the part of the orbit with the lowest velocity, thus it is the best place to perform inclination changes. Thirdly, Burn 3 is a combination of these two burns. Since an inclination change burn is performed at an angle to the velocity vector and a raising burn is performed parallel to the velocity vector, performing both at the same time is more efficient than performing them individually for the same reasoning as above regarding vector addition.

Each of the 2 Burn Method's burns carry a degree of efficiency and inefficiency. Burn 1 is efficient through its use of the Oberth Effect, and it selects the higher ascending/descending node to get the maximum benefit from this. However, as it does not establish the full apoapsis of the asteroid's orbit, this must be done later in Burn 2, where it will be more costly to raise the apoapsis. Burn 2 is difficult to judge, as it combines several burns in a single burn (setting the apoapsis, setting the periapsis, and adjusting the inclination) gaining efficiency through the vector addition theorem, as well as fixing the inclination in a single burn as opposed to the two burns used in the 3 Burn Method. However, Burn 2 does not set the Apoapsis at the Periapsis and vice versa, leading to inefficiency in kinetic energy gain. These differences between the two Methods are beneficial to the investigation because using them together decreases the average Delta-V of the dataset by 9% compared to the 3 Burn Method alone, and by 1% when compared to the 2 Burn Method alone.

7. Results and Analysis

7.1. Delta-V Distribution: All Objects

The MPC dataset contains all known small bodies in the solar system, including comets, NEOs, KBOs , Trojans, and other bodies. For this paper, we define:

- *NEOs* have a periapsis less than the semimajor axis of Mars. Although NEOs may not be near the Earth for their entire orbit, they are nearby at periapsis.
- *Main Belt* objects have their orbit entirely contained within Mars' and Jupiter's semimajor axes
- *Outer* objects have an apoapsis greater than the semimajor axis of Jupiter and a periapsis greater than the semimajor axis of Mars, thus passing outside of the Main Belt during their orbits.

Table 1 shows the contents of the MPCORB dataset broken down by type.

Table 1: MPC Objects

Object Class	Periapsis	Apoapsis	Objects	Median Delta-V
NEOs	$< a_{Mars}$	$< a_{Mars}$	19743	9.6 km s^{-1}
Main Belt	$> a_{Mars}$	$< a_{Jup}$	691026	10.0 km s^{-1}
Outer	$> a_{Mars}$	$> a_{Jup}$	9636	12.0 km s^{-1}
Total	–	–	720405	10.0 km s^{-1}

Figure 17 plots the Delta-V distributions of these four classes of objects. The most direct correlation in Figure 17 is that Delta-V scales with semimajor axis. This is expected from orbital mechanics and is no surprise. The trailing end of the NEOs is likely due to NEOs with orbits inside of Earth's, near the Sun, a regime that our burn methods are not designed for.

7.2. Delta-V Distribution: Main Belt

The purpose of this project is to analyze the orbits of the Main Belt asteroids and determine the feasibility of deploying mining missions to these objects.

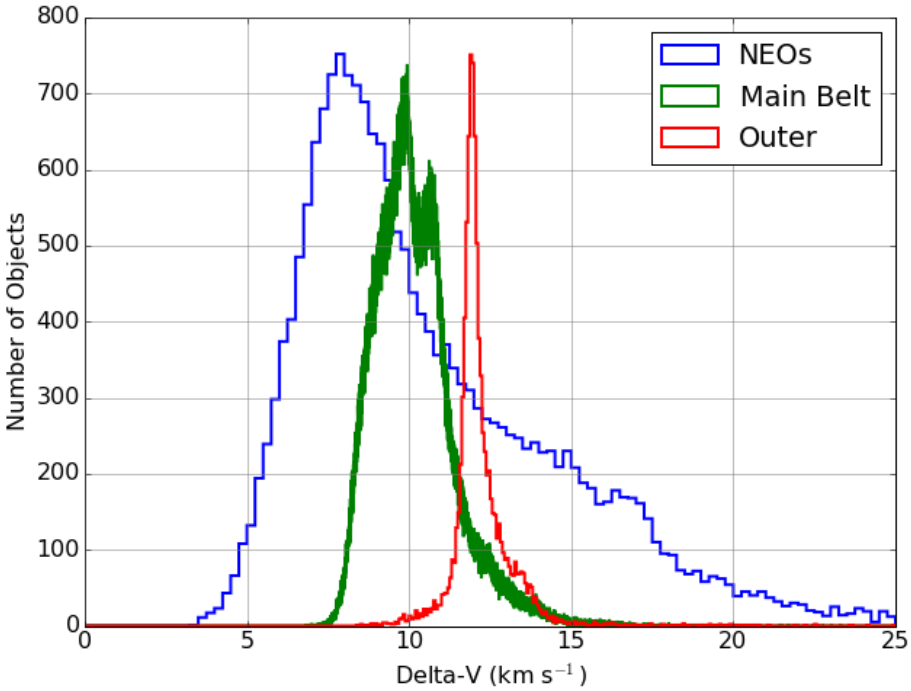

Figure 17: The distribution of asteroid Delta-V in the dataset, using the lowest value from the two methods per asteroid. The peaks of each dataset are scaled to a similar height by binning. The Main Belt has 10,000 bins, the NEOs have 100 bins, and the Outer objects have 400 bins.

Figures 18 and 19 show that a spacecraft with a Delta-V rating of 10.0 km s^{-1} can rendezvous with half of the Main Belt asteroids.

Looking more closely at the low Delta-V Main Belt asteroids (see Figure 20), there are 5,211 targets within 8 km s^{-1}, 214 targets within 7.5 km s^{-1}, and just 6 targets within 7 km s^{-1}. The number of accessible Main Belt Asteroids exceeds the number of accessible NEOs at Delta-V $\approx$ 8.0 km s^{-1}. This demonstrates that there are plenty of potential asteroid targets for research and mining, but there is a threshold Delta-V that must be reached for the Main Belt asteroids to be accessible targets.

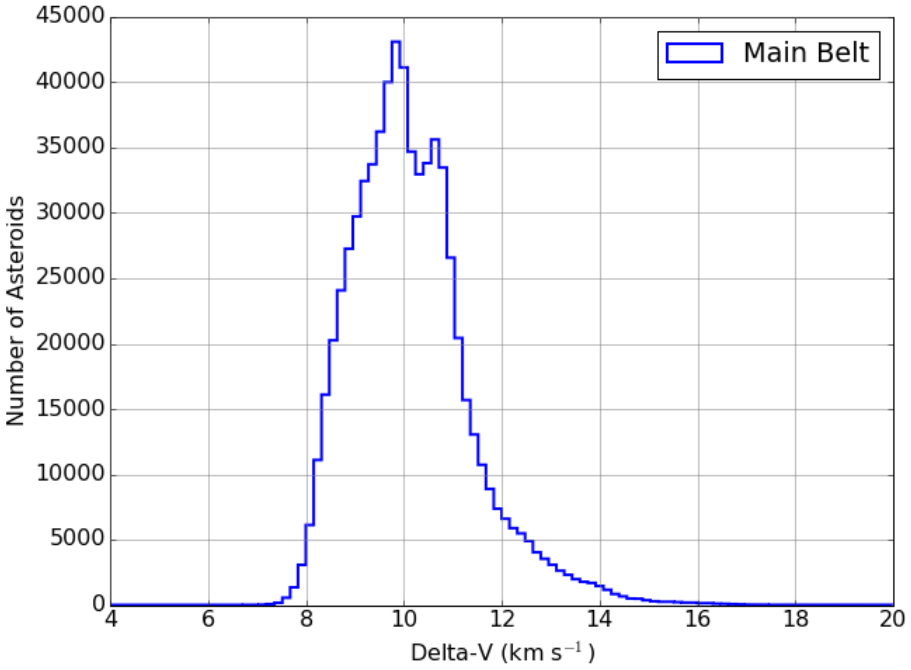

Figure 18: The distribution of asteroid Delta-V in the dataset, using the lowest value for Delta-V from the two methods per asteroid.

7.3. Low Delta-V Orbital Parameters

The completed dataset can provide insight into the types of orbits that are most accessible, and can be used to analyze the strengths and weaknesses of each method of orbital burns. The distribution of Delta-V in (a, i) space is shown in Figure 21.

Clearly Delta-V is minimized in orbits with $a < 2.5$ AU, and $i < 10°$. These orbits are the most similar to that of the Earth and are thus the lowest Delta-V targets.

Even at distances near Jupiter (a=5.2 AU), at $i < 15°$ the Delta-V does not exceed $\sim$13 km s^{-1}. This is because at high semimajor axis a Delta-V approaches the solar escape velocity from Earth's solar orbit (42.1 km s^{-1}).

Instead, high inclination is much more costly to reach, equaling 13 km s^{-1} by $i \approx 25°$ and climbing to $\sim$16 km s^{-1} by $i \approx 30°$.

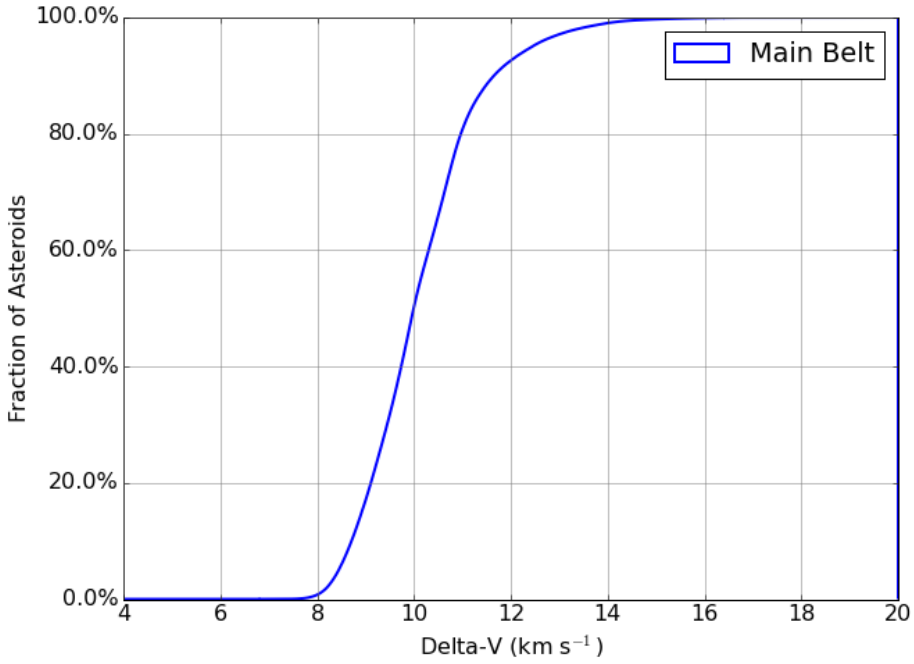

Figure 19: Integral plot of the fraction of Main Belt asteroids that can be reached for a given Delta-V, using the lowest value for Delta-V from the two methods per asteroid. Note the small tail of $\Delta V) < 8$ km s^{-1} objects.

The argument of periapsis also has a significant effect on Delta-V. Figure 22 shows that both orbital methods prefer the argument of the periapsis to be either at 0° or 180°. These argument of periapsis values result in a minimal Burn 2 of the 3 Burn Method, and would allow Burn 2 of the 2 Burn Method to occur at the apoapsis, the most efficient place for it to occur. By the inverse reasoning, arguments of the periapsis of 90° and 270° are highly unfavorable for both methods. On average in the dataset, orbits with $\omega = 180° \pm 20°$ have a Delta-V that is 1.1 km s^{-1} lower than orbits with $\omega = 90° \pm 20°$.

7.4. The Lowest Delta-V Main Belt Asteroids

This study is not purely statistical. We have identified specific low Delta-V Main Belt objects. Table 2 lists some properties of the 10 Main Belt asteroid with the lowest Delta-V.

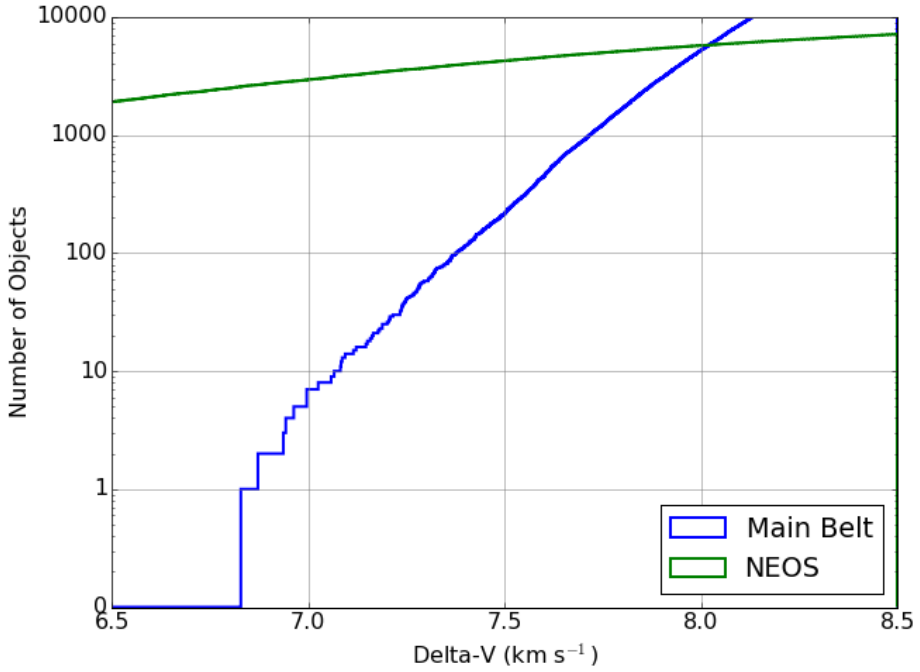

Figure 20: Logarithmic integral plot of Main Belt asteroids and NEOs that can be reached for a given Delta-V, using the lowest value for Delta-V from the two methods per asteroid.

Table 2: 10 Lowest Delta-V Objects

Designation	ω (°)	i (°)	e	a (AU)	Delta-V	Method	H-mag
P7471	201.79536	1.64067	0.05768	1.72553	6.94 km s^{-1}	2	19.4
R1774	351.99342	1.55672	0.14794	1.82854	6.83 km s^{-1}	2	18.9
X9147	196.51032	0.38700	0.17064	1.93272	7.03 km s^{-1}	1	18.7
d6707	211.45293	4.03677	0.03018	1.62904	7.00 km s^{-1}	2	20.0
K06T09G	157.85926	0.51266	0.18357	1.89659	6.87 km s^{-1}	1	19.4
K16CD7U	312.03544	0.83988	0.20963	1.93816	7.06 km s^{-1}	1	19.5
K01FL1A	242.51722	0.31751	0.26329	2.08645	7.07 km s^{-1}	1	21.8
K05Q53U	202.12606	0.09758	0.27036	2.11243	7.00 km s^{-1}	1	19.1
K06O27D	4.57879	1.15080	0.18180	1.97099	7.08 km s^{-1}	2	20.8
K10JC9H	189.98297	3.08198	0.01223	1.64215	6.94 km s^{-1}	2	–

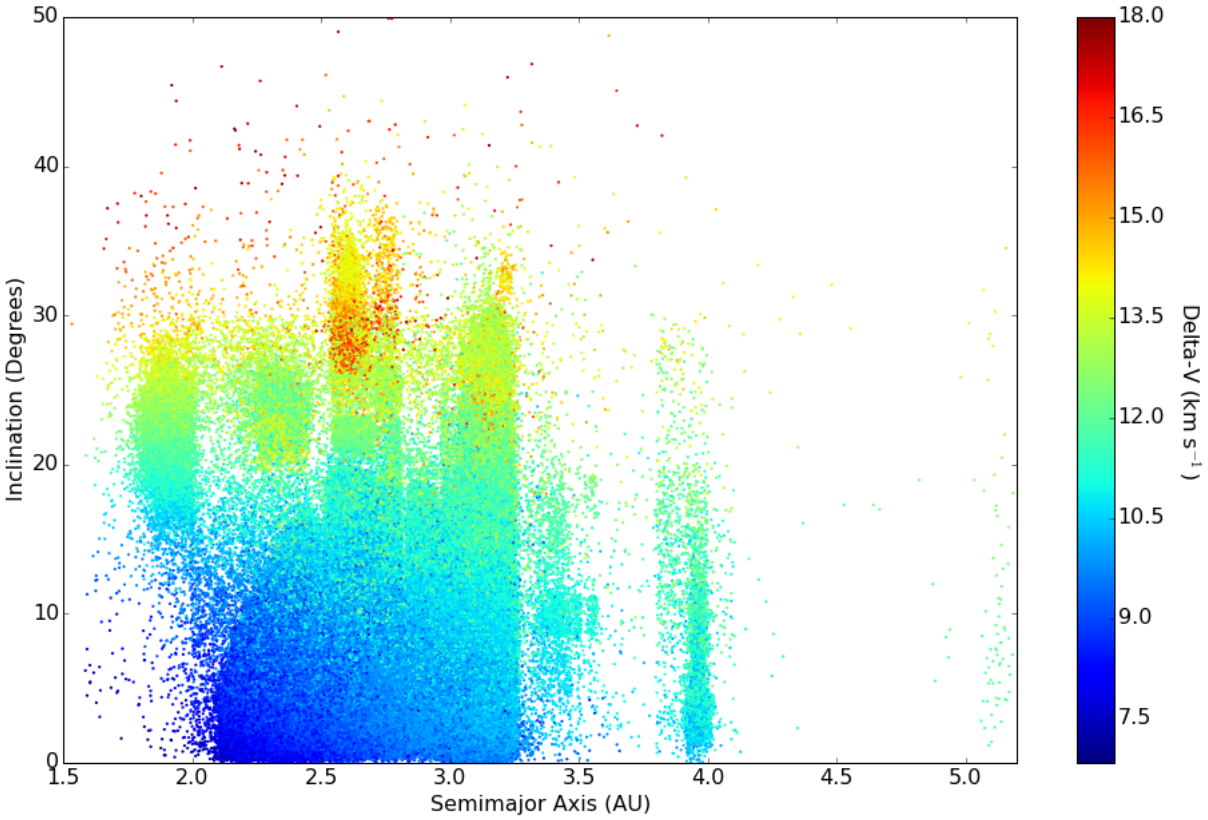

Figure 21: Asteroid inclination plotted against semimajor axis (a), with Delta-V in km s^{-1} as a color scale. Asteroids with a Delta-V of 18 km s^{-1} or greater are not included on this plot. These objects make up $< 1\%$ of the dataset.

7.5. Current Mission Feasibility

To test the practicality of the results, we propose a hypothetical mission using the Atlas V 551 to rendezvous with Main Belt asteroid 9283 "MartinElvis." The parameters of "MartinElvis" are listed in Table 3.

Table 3: "MartinElvis" Parameters

Designation	ω (°)	i (°)	e	a (AU)	Delta-V	Method	H-mag
09283	247.08651	2.23369	0.15893	2.45411	9.33 km s^{-}1	1	14.4

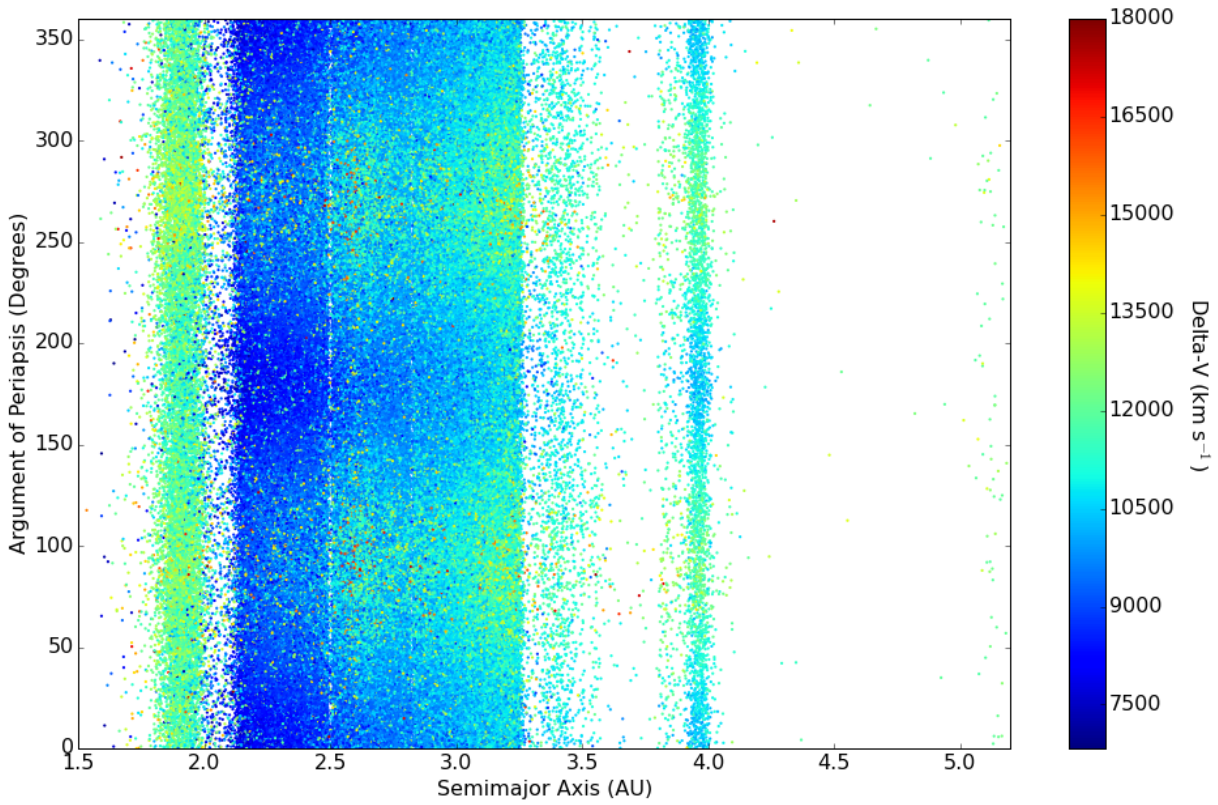

Figure 22: Asteroid argument of the periapsis ω plotted against semimajor axis a, with Delta-V in km s^{-1} as a color scale.

"MartinElvis" is a representative sample of a Main Belt asteroid, as the asteroid's Delta-V (9.33 km s^{-}1) is slightly below the median Delta-V of the Main Belt (10.0 km s^{-1}). The 3 Burn Method is preferred for "MartinElvis." To test the mission feasibility, we choose the Atlas V 551 as the launch vehicle. "MartinElvis" has an apoapsis of 2.84 AU, thus the semimajor axis of the 3 Burn transfer orbit would be 1.92 AU (see Eq. (14)). Combining Eq. (10), (12), and (15) and solving for C3 gives:

$$\text{C3} = \left(\sqrt{\mu \left(\frac{2}{r_\oplus} - \frac{1}{a_t} \right)} - v_\oplus \right)^2 \tag{61}$$

This corresponds to a C3 of 41 km^2 s^{-2} for "MartinElvis."

Using Atlas V 551 payload ratings as function of C3 [12], the Atlas V 551 can launch a mass of 3140 kg to a C3 of 41 km^2 s^{-2}. This uses the Atlas V 551 to perform the entirety of Burn 1. The 3140 kg spacecraft must then perform burns 2 and 3. The Delta-V of burns 2 and 3 are 0.88 km s^{-1} and 3.52 km s^{-1} respectively, for a total remaining Delta-V of 4.40 km s^{-1}.

Returning to the rocket equation (Eq. (2)), we choose v_e to be 4.4 km s^{-1}, the value for the RL-10 and J2X LH2/LOX engines [5]. Using these values, we solve for the delivered mass m_f to "MartinElvis".

$$\frac{m_i}{m_f} = \exp\left(\frac{\Delta V}{v_e}\right) \qquad \frac{3140 \text{ kg}}{m_f} = \exp\left(\frac{4.40 \text{ km s}^{-1}}{4.4 \text{ km s}^{-1}}\right) \tag{62}$$

$$m_f = 1155 \text{ kg} \tag{63}$$

This is a promising result, as the Rosetta Orbiter had a dry mass of 1180 kg [7]. For a full mining mission, this would be insufficient, but "MartinElvis" is not a low Delta-V Main Belt mining target.

This type of exercise could be largely expanded upon in future studies, creating a database of delivered payloads to asteroids using different launch vehicles (see Section 8.2: Future Directions).

8. Conclusions and Future Directions

8.1. Conclusions

This examination of Main Belt asteroids as prospective targets for mining missions has produced promising results. Within a Delta-V of 8 km s^{-1}, starting from LEO, one can access 5,211 asteroid targets. Additionally, there are 214 targets that can be reached with a Delta-V of less than 7.5 km s^{-1}. This gives a fantastic selection of potential targets for early mining missions. Additionally, the development of two very different sets of orbital burns that can be used for rendezvous are excellent tools for further orbital applications.

This investigation concludes that the asteroid mining industry has a substantial number of feasible targets in the Main Belt that can be used for both commercial and scientific initiatives in the near future.

8.2. Future Directions

This project simply lays the groundwork for mining analysis of the Main Belt. We plan to annotate the orbital calculation code and publish it as a tool for the scientific community, along with the output data formatted into an online database for public use. Follow up projects could include cross referencing this dataset with Main Belt asteroid size and composition to further focus on optimal mining targets. An expansion of the orbital code should investigate launch windows for given allowed increases in Delta-V.

The next steps in this project involve the application of its results. The round trip journey time is an important constraint, given the time cost of mining. The synodic periods of the asteroids constrain both launch opportunities and the and the chances to better characterize potential targets. Another constraint is the comparison of the results to specific rocket systems specifications to estimate the deliverable payload with current and future hardware. Each of these constraints will refine, but also restrict the optimum target list.

9. Acknowledgements

A special thanks to Dr. Martin Elvis and Dr. Jonathan McDowell for their advising and great contributions to this project.

Thank you to Dr. Matthew Holman for his remarks and input during this paper's development.

This research has made use of data and/or services provided by the International Astronomical Union's Minor Planet Center.

10. References

[1] Adams, R., Richardson, G. "Using the Two-Burn Escape Maneuver for Fast Transfers in the Solar System and Beyond" NASA Archives. Retrieved 06 Dec. 2016.

[2] Coverstone-Carroll, V., Hartmann, J.W., Mason, W.J. 1999, "Optimal multi-objective low-thrust spacecraft trajectories" Computer Methods in Applied Mechanics and Engineering. 186 (2000) 387402

[3] Dobson, W., Huff, V., Zimmerman, A. 1962, "Elements and Parameters of the Osculating Orbit and Their Derivatives" NASA Technical Note D-1106

[4] Elvis, Martin 2003, "Prospecting Asteroid Resources", *Asteroids: Prospective Energy and Material Resources*, Viorel Badescu, Springer-Verlag Berlin Heidelberg, New York

[5] Elvis, M., McDowell, J. et al. 2011, "Ultra-low delta-v objects and the human exploration of asteroids", Planetary & Space Science, 59, 1408-1412

[6] Forward, Robert L. 1995, "A Transparent Derivation of the Relativistic Rocket Equation" 31st AIAA Joint Propulsion Conference and Exhibit

[7] Glassmeier, K et al. 2006, "The Rosetta Mission: Flying Towards The Origin Of The Solar System" Space Science Reviews (2007) 128: 1?21

[8] Hohmann, W. 1925, "Die Errichbarkeit der Himmelskorper: Untersuchungen uber das Raumfahrtproblem" (R. Oldenbourg, Munich). English translation: The Availability of Heavenly Bodies, NASA report NASA-TT-F-44 (1960)

[9] NASA 2016, "Ceres: By the numbers" Solar System Exploration. http://solarsystem.nasa.gov/planets/ceres/facts Retrieved 06 Dec. 2016.

[10] Scheck, Florian A. 1999, *Mechanics: From Newton's Laws to Deterministic Chaos*. Springer-Verlag Berlin Heidelberg, New York

[11] Shoemaker, E.M., Helin, E.F. 1978, "Asteroids: an Exploration Assessment" NASA CP-2053, pp. 245-256

[12] Wise, M., Lafleur, J., Saleh, J. 2010, "Regression Analysis Of Launch Vehicle Payload Capability For Interplanetary Missions" IAC-10.D2.P06.

Appendix A. 3 Burn Method Code

```
import math
import numpy as np

np.set_printoptions(formatter={'float':'{:g}'.format}) #specifies
    ↪ numpy array number format

#Constants and Unit Conversion
G=6.67408*10**(-11) #m^3 kg^-1 s^-2
Msun=1.988*10**30 #kg
u=Msun*G
MEarth=5.9722*10**24 #kg
ue=MEarth*G
REarth=149.6*10**9 #meters
VEarth=math.sqrt(u*(float(2)/float(REarth)-float(1)/float(REarth)))
Vpark=math.sqrt(ue*(float(2)/float(6378000+100000)-float(1)/float
    ↪ (6378000+100000))) #orbital velocity at 100km parking orbit
Vesc=math.sqrt(2*ue/(6378000+100000)) #escape velocity at 100km
    ↪ parking orbit
def MtoAU(m):
    return m*6.68459*10**(-12)
def AUtoM(AU):
    return AU/(6.68459*10**(-12))
def DegtoRad(deg):
    return deg*math.pi/float(180)
def RadtoDeg(rad):
    return rad*180/math.pi

#Final Function
def DeltaV(w,i,ec,a):
    Total=M1(ec,AUtoM(a))+M2(DegtoRad(w),DegtoRad(i),ec,AUtoM(a))+
        ↪ M3(DegtoRad(w),DegtoRad(i),ec,AUtoM(a))
    return Total
def DeltaVexp(w,i,ec,a):
    return M1(ec,AUtoM(a)),M2(DegtoRad(w),DegtoRad(i),ec,AUtoM(a)),
        ↪ M3(DegtoRad(w),DegtoRad(i),ec,AUtoM(a))
def DVArray(array):
    return DeltaV(array[0],array[1],array[2],array[3])
```

```
#Maneuver 1
#Start at 100 km Earth parking orbit
def AstAp(ec,a): #apoapsis of asteroid
    return (1+ec)*a
def AstPe(ec,a): #periapsis of asteroid
    return (1-ec)*a
def velo(semi,r): #orbital velocity at a radius
    return math.sqrt(u*(float(2)/float(r)-float(1)/float(semi)))
def TransPeV(ec,a): #velocity at transfer periapsis
    return velo((AstAp(ec,a)+REarth)/float(2),REarth)
def M1(ec,a): #Delta-V for Maneuver 1
    return math.sqrt(((TransPeV(ec,a)-VEarth)**2)+(Vesc**2))-Vpark

#Maneuver 2
def TransA(ec,a):
    return (AstAp(ec,a)+REarth)/float(2)
def TransEC(ec,a): #Transfer orbit Eccentricity
    return float((AstAp(ec,a)-REarth))/(AstAp(ec,a)+REarth)
def perilat(w,i): #"Latitude" of Periapsis
    return math.asin(math.sin(w)*math.sin(i))
def TransR(ec,a): #Radius at Maneuver 2 burn
    return TransA(ec,a)*(1-TransEC(ec,a)**2)
def FPAngle(ec,a): #Flight Path Angle
    return math.acos(REarth*TransPeV(ec,a)/(TransR(ec,a)*velo(
        ↪ TransA(ec,a),TransR(ec,a))))
def M2Angle(w,i,ec,a): #Maneuver 2 Angle
    return math.acos(math.cos(perilat(w,i))*(math.cos(FPAngle(ec,a)
        ↪ )**2)+(math.sin(FPAngle(ec,a))**2))
def M2(w,i,ec,a): #Delta-V for Maneuver 2, derived from law of
    ↪ cosines with equal side lengths
    return 2*velo(TransA(ec,a),TransR(ec,a))*math.sin(M2Angle(w,i,
        ↪ ec,a)/2)

#Maneuver 3
def TwistAng(w,i): #angle for very last maneuver
    #Function exhibits odd behavior near limiting case of pi/2 for
        ↪ inclination
```

```
    #This is expected, as the orbital approach is designed for
        ↪ inclinations below 45 degrees
    return math.acos(math.cos(i)/math.sqrt((math.cos(w)**2)+((math.
        ↪ cos(i)**2)*(math.sin(w)**2))))
def M3Vi(ec,a): #initial velocity at Maneuver 3 position
    return velo(TransA(ec,a),AstAp(ec,a))
def M3Vf(ec,a): #final velocity at Maneuver 3 position
    return velo(a,AstAp(ec,a))
def M3(w,i,ec,a): #Delta-V for Maneuver 3, derived from law of
    ↪ cosines
    return math.sqrt(M3Vi(ec,a)**2+M3Vf(ec,a)**2-2*M3Vi(ec,a)*M3Vf(
        ↪ ec,a)*math.cos(TwistAng(w,i)))

#Load datafile, line 42 is data, skip_header=41
DATA=np.genfromtxt('MPCORB_import.DAT',delimiter=None,skip_header
    ↪ =41,usecols=(5,7,8,10))
NAMES=np.genfromtxt('MPCORB_import.DAT',dtype='string',delimiter=
    ↪ None,skip_header=41,usecols=(0))
print 'Import Successful'

#Calculate Delta-V and Output Datafile
Result=np.apply_along_axis(DVArray,1,DATA,)
ResultTable=np.transpose(np.append(np.transpose(DATA),[Result],axis
    ↪ =0))
ResW=ResultTable[:,0]
ResI=ResultTable[:,1]
ResEC=ResultTable[:,2]
ResA=ResultTable[:,3]
ResDV=ResultTable[:,4]
FinalDataTable=np.array(zip(NAMES, ResW, ResI, ResEC, ResA, ResDV),
    ↪  dtype=[('NAMES', 'S16'), ('ResW', float), ('ResI', float),
    ↪ ('ResEC', float),('ResA',float),('ResDV',float)])
np.savetxt('DeltaV_Results.txt',FinalDataTable, fmt=["%s",]+["%.5f"
    ↪ ,]*5)
```

Appendix B. 2 Burn Method Code

```
import math
import numpy as np

np.set_printoptions(formatter={'float':'{:g}'.format}) #specifies
    ↪ numpy array number format

#Constants and Unit Conversion
G=6.67408*10**(-11) #m^3 kg^-1 s^-2
Msun=1.988*10**30 #kg
u=Msun*G
MEarth=5.9722*10**24 #kg
ue=MEarth*G
REarth=149.6*10**9 #meters
VEarth=math.sqrt(u*(float(2)/float(REarth)-float(1)/float(REarth)))
def MtoAU(m):
    return m*6.68459*10**(-12)
def AUtoM(AU):
    return AU/(6.68459*10**(-12))
def DegtoRad(deg):
    return deg*math.pi/float(180)
def RadtoDeg(rad):
    return rad*180/math.pi

#Final Function
def DeltaV(w,i,ec,a):
    return M1(DegtoRad(w),ec,AUtoM(a))+M2(DegtoRad(w),DegtoRad(i),
        ↪ ec,AUtoM(a))
def DeltaVexp(w,i,ec,a):
    return M1(DegtoRad(w),ec,AUtoM(a)),M2(DegtoRad(w),DegtoRad(i),
        ↪ ec,AUtoM(a))
def DVArray(array):
    return DeltaV(array[0],array[1],array[2],array[3])

#Asteroid Parameters
def AstAp(ec,a): #apoapsis of asteroid
    return (1+ec)*a
def AstPe(ec,a): #periapsis of asteroid
```

```
    return (1-ec)*a

#Maneuver 1
#Start at 100 km Earth parking orbit
ParkAlt=100000 #Earth Parkign Orbit altitude above planet surface
Vpark=math.sqrt(ue*(float(2)/float(6378000+ParkAlt)-float(1)/float
    ↪ (6378000+ParkAlt))) #orbital velocity at Earth parking orbit
Vesc=math.sqrt(2*ue/(6378000+ParkAlt)) #escape velocity at Earth
    ↪ parking orbit
def velo(semi,r): #orbital velocity at a radius
    return math.sqrt(u*(float(2)/float(r)-float(1)/float(semi)))
def RNode(w,ec,a): #radius at ascending or decending node, choose
    ↪ higher one
    Node1=a*(1-(ec**2))/(1+ec*math.cos(-w))
    Node2=a*(1-(ec**2))/(1+ec*math.cos(math.pi-w))
    if Node1>Node2:
        return Node1
    else:
        return Node2
def NodeChoice(w,ec,a): #which node was chosen, for all future
    ↪ calculation the periapsis direction is defined as 0 degrees
    Node1=a*(1-(ec**2))/(1+ec*math.cos(-w))
    Node2=a*(1-(ec**2))/(1+ec*math.cos(math.pi-w))
    if Node1>Node2:
        return -w
    else:
        return math.pi-w
def TransPeV(w,ec,a): #velocity at transfer periapsis
    return velo((RNode(w,ec,a)+REarth)/float(2),REarth)
def M1(w,ec,a): #Delta-V for Maneuver 1
    return math.sqrt(((TransPeV(w,ec,a)-VEarth)**2)+(Vesc**2))-
        ↪ Vpark

#Maneuver 2
#Define Orbital Elements
def TransA(w,ec,a):
    return (RNode(w,ec,a)+REarth)/float(2)
def TransEC(w,ec,a): #Transfer orbit Eccentricity
```

```
    return float((RNode(w,ec,a)-REarth))/(RNode(w,ec,a)+REarth)
def AstB(ec,a): #semiminor axis of asteroid orbit
    return a*math.sqrt(1-ec**2)
def AstC(ec,a): #"c" of ellipse, useful for calculation
    return a*ec
#Define Velocity magnitudes
def TransVM2(w,ec,a):
    return velo(TransA(w,ec,a),TransA(w,ec,a)*(1+TransEC(w,ec,a)))
def AstVM2(w,ec,a):
    return velo(a,RNode(w,ec,a))
#Define Vector components
def VecX(w,ec,a): #X direction vector component of asteroid orbit
    ↪ at node
    return -RNode(w,ec,a)*math.sin(NodeChoice(w,ec,a))/AstB(ec,a)
        ↪ **2
def VecY(w,ec,a): #Y direction vector component of asteroid orbit
    ↪ at node
    return (RNode(w,ec,a)*math.cos(NodeChoice(w,ec,a))+AstC(ec,a))/
        ↪ a**2
def NormConstAst(w,ec,a):#Normalization constant for Velocity
    ↪ vector
    return math.sqrt(VecX(w,ec,a)**2+VecY(w,ec,a)**2)
def VecXTrans(w,i,ec,a): #X direction vector component of transfer
    ↪ orbit at node
    return -math.sin(NodeChoice(w,ec,a))*math.cos(i)
def VecYTrans(w,i,ec,a): #Y direction vector component of transfer
    ↪ orbit at node
    return math.cos(NodeChoice(w,ec,a))*math.cos(i)
def VecZTrans(i):
    return math.sin(i)
def TransNorm(w,i,ec,a):
    return math.sqrt(VecXTrans(w,i,ec,a)**2+VecYTrans(w,i,ec,a)**2+
        ↪ VecZTrans(i)**2)

def FinalM2Angle(w,i,ec,a): #Calculate Angle between Orbits using
    ↪ Dot Product
    return math.acos((VecX(w,ec,a)*VecXTrans(w,i,ec,a)+(VecY(w,ec,a
        ↪ )*VecYTrans(w,i,ec,a)))/(NormConstAst(w,ec,a)*TransNorm(
```

```
        ↪ w,i,ec,a)))
def M2(w,i,ec,a): #Delta-V for Maneuver 1, derived from law of
    ↪ cosines
    return math.sqrt(TransVM2(w,ec,a)**2+AstVM2(w,ec,a)**2-2*
        ↪ TransVM2(w,ec,a)*AstVM2(w,ec,a)*math.cos(FinalM2Angle(w,
        ↪ i,ec,a)))

#Load datafile, line 42 is data, skip_header=41
DATA=np.genfromtxt('MPCORB_import.DAT',delimiter=None,skip_header
    ↪ =41,usecols=(5,7,8,10))
NAMES=np.genfromtxt('MPCORB_import.DAT',dtype='string',delimiter=
    ↪ None,skip_header=41,usecols=(0))
print 'Import Successful'

#Calculate Delta-V and create output file
Result=np.apply_along_axis(DVArray,1,DATA)
ResultTable=np.transpose(np.append(np.transpose(DATA),[Result],axis
    ↪ =0))
ResW=ResultTable[:,0]
ResI=ResultTable[:,1]
ResEC=ResultTable[:,2]
ResA=ResultTable[:,3]
ResDV=ResultTable[:,4]
FinalDataTable=np.array(zip(NAMES, ResW, ResI, ResEC, ResA, ResDV),
    ↪  dtype=[('NAMES', 'S16'), ('ResW', float), ('ResI', float),
    ↪ ('ResEC', float),('ResA',float),('ResDV',float)])
np.savetxt('DeltaV_Results.txt',FinalDataTable, fmt=["%s",]+["%.5f"
    ↪ ,]*5)
```

Appendix C. Data Combination Code

```
import numpy as np
import math

#Find best method for each datapoint
OLD=np.genfromtxt('DeltaV_Results_Method1.txt',delimiter=None,
    ↪ usecols=(5))
OLDFULL=np.genfromtxt('DeltaV_Results_Method1.txt',delimiter=None)
NEW=np.genfromtxt('DeltaV_Results.txt',delimiter=None,usecols=(5))
NAMES=np.genfromtxt('MPCORB_import.DAT',dtype='string',delimiter=
    ↪ None,skip_header=41,usecols=(0))
DATA=np.vstack((OLD, NEW)).T
def best(array):
    if array[1]>array[0]:
        return array[0],1
    else:
        return array[1],2
MinResult=np.apply_along_axis(best,1,DATA)

#Create final output datafile
BEST=MinResult[:,0]
Method=MinResult[:,1]
ResW=OLDFULL[:,1]
ResI=OLDFULL[:,2]
ResEC=OLDFULL[:,3]
ResA=OLDFULL[:,4]
DV1=OLDFULL[:,5]
CombinedDataTable=np.array(zip(NAMES, ResW, ResI, ResEC, ResA, DV1,
    ↪ NEW, BEST, Method), dtype=[('NAMES', 'S16'), ('ResW', float
    ↪ ), ('ResI', float), ('ResEC', float),('ResA',float),('DV1',
    ↪ float),('NEW',float),('BEST',float),('Method',int)])
np.savetxt('DeltaV_Combined_Results.txt',CombinedDataTable, fmt=["%
    ↪ s",]+["%.5f",]*2+["%.7f",]*2+["%.2f",]*3+["%.0f",])
```